

Robust H_∞ kinematic control of manipulator robots using dual quaternion algebra

L.F.C. Figueredo, B.V. Adorno, *Senior Member, IEEE*, J.Y. Ishihara

Abstract—This paper proposes a robust dual-quaternion based H_∞ task-space controller for robot manipulators. To address the manipulator liability to modeling errors, uncertainties, exogenous disturbances, kinematic singularities, and their influence upon the kinematics of the end-effector pose (i.e., position and orientation), we adapt H_∞ techniques—suitable only for additive noises—to unit dual quaternions. The noise to error attenuation within the H_∞ framework has the additional advantage of casting aside requirements concerning noise distributions, which are significantly hard to characterize within the group of rigid body transformations. Using dual quaternion algebra, we provide a connection between performance effects over the end-effector trajectory and different sources of uncertainties and disturbances while satisfying attenuation requirements with minimum instantaneous control effort. The result is an easy-to-implement closed form H_∞ control design criterion. The H_∞ conditions derived in this paper are extended to conceive a new kinematic singularity avoidance technique suitable for the proposed non-Euclidean task-space manifold, which ensures proper behavior throughout the task space. The effectiveness and performance overview of the proposed strategies are evaluated within different realistic simulated scenarios.

Index Terms— H_∞ control, kinematic control, unit dual quaternions, robust control, singularity avoidance

I. INTRODUCTION

The last few decades have seen an increasing interest in the extension of the robotics domain from controlled industry environments to human-centered ones. This new generation of robots is expected to execute tasks, potentially alongside humans, deployed at increasingly less controlled scenarios and contexts where robustness and reactivity become crucial features. This way, there is a paradigm shift towards the development of robots that are intrinsically safe, whose controllers are designed to enhance performance [1]. As a consequence, kinematic controllers, which are prevalent in industry and usually assume stiff manipulators working at relatively low velocities and accelerations [2], behave poorly when implemented on such intrinsically safe, compliant, robots. On the

other hand, kinematic controllers are simple to implement and do not require the specification of the robot's inertial parameters. In addition, physical human-robot interactions usually *do* happen at low velocities and accelerations, hence a kinematic controller that works well on both standard industrial robots and compliant robots would be of great value. Such a controller must be robust to modeling errors and uncertainties, exogenous disturbances, kinematic singularities, and even possible representational singularities inherent to the representation used for the description of the end-effector pose.

To cope with the challenges that arise from the pose description and possible representation singularities, the coupled translation and rotation kinematics can be modeled using non-minimal representations such as homogeneous transformation matrices (HTM) and unit dual quaternions. The *unit* dual quaternion is a non-singular representation for rigid transformations that is more compact, efficient and less computationally demanding than HTM [3]–[5]. In addition, dual quaternions have strong algebraic properties and can be used to represent rigid motions, twists, wrenches and several geometrical primitives—e.g., Plücker lines, planes—in a very straightforward way [6], [7]. Moreover, control laws are defined directly over a vector field, eliminating the need to extract additional parameters or to design matrix-based controllers.

Thanks to those advantages, there has been an increasing interest in the study of kinematic representation and control in dual quaternion space. Those works comprise rigid body motion stabilization, tracking, and multiple body coordination [8]–[12], and kinematic control of manipulators with single and multiple arms and human-robot interaction [13]–[15].

Most of the existing results designed for rigid body motion control, using dual quaternion algebra, are based on a logarithmic mapping and its relation to Lie algebra, which promptly connects translation and orientation errors to the feedback control gains. Nonetheless, these results are usually restricted to unconstrained rigid bodies (i.e., free flying robots), thus neglecting the specificities inherent to the manipulator description and its kinematic chain. This is especially relevant for manipulator robots because usually the task is defined in the task-space (i.e., at the end-effector level), but the control inputs are defined in the joint space. Since the mapping between the end-effector generalized velocities and the control inputs (i.e., the joints velocities) is done by means of a Jacobian matrix, controllers designed for unconstrained rigid bodies—which usually provide (generalized) velocity inputs for the rigid bodies—must ensure that the rigid-body velocity inputs belong to the range space of the Jacobian matrix. This can be guaranteed only if the manipulator robot is not

L.F.C. Figueredo is with the Graduate Program in Electrical Engineering (PPGEE) of the Federal University of Minas Gerais (UFMG), 31270-010, Belo Horizonte-MG, Brazil (figueredo@ieee.org).

B.V. Adorno is with the Federal University of Minas Gerais (UFMG), Department of Electrical Engineering, 31270-010, Belo Horizonte-MG, Brazil (adorno@ufmg.br).

J.Y. Ishihara is with the Universidade de Brasília (UnB), Automation and Robotics Laboratory, Brasília-DF (ishihara@unb.br).

This work was supported by CNPq, CAPES, FAPEMIG, and by the project INCT (National Institute of Science and Technology) under the grant CNPq (Brazilian National Research Council) 465755/2014-3, FAPESP (São Paulo Research Foundation) 2014/50851-0.

underactuated nor at a singular configuration.

Furthermore, despite the aforementioned advantages of the unit dual quaternion representation, there is a gap in existing literature concerning the influence of control parameters, uncertainties, and disturbances—including those caused by kinematic singularities (i.e., when the Jacobian matrix loses rank)—over the robustness and performance of the end-effector trajectory tracking, when the trajectory is represented by unit dual quaternions.

In this context, this paper proposes a robust dual-quaternion based H_∞ task-space controller for robot manipulators. To address the manipulator liability to modeling errors, uncertainties, exogenous disturbances, kinematic singularities, and their influence upon the kinematics of the end-effector pose (i.e., position and orientation), we adapt H_∞ techniques—suitable only for additive noises—to unit dual quaternions. The new method provides a direct connection between different sources of uncertainties and disturbances and the corresponding performance effects over the end-effector trajectory. The proposed dual quaternion kinematic controller explicitly addresses the influence of such disturbances over the end-effector pose, in the H_∞ sense, which has the advantage of casting aside requirements regarding detailed knowledge about the statistical distribution of disturbances—which are significantly hard to characterize within the group $\text{Spin}(3) \times \mathbb{R}^3$ of unit dual quaternions (or even $SE(3)$). Using dual quaternion algebra, we derive easy-to-implement closed form H_∞ control and tracking strategies at the end-effector level that incorporate robustness requirements, disturbance attenuation and performance properties over the translation and rotational kinematics, while minimizing the required control effort.

As another contribution to the state-of-the-art, we also derive a novel singularity-avoidance technique by extending the proposed H_∞ control strategy. Since avoidance techniques in the context of inescapable singularities inherently modify the transient trajectory [16]–[19], we characterize singularities as a disturbance to the system. This way, H_∞ performance conditions enables us to take advantage of well-developed H_∞ norm properties to derive a suitable control law that easily bounds the worst-case influence of kinematic singularities over the time-varying unit dual quaternion that represents the end-effector trajectory.

In summary, the paper contributions with respect to the state of the art are:

- 1) Development of a novel, easy-to-implement, closed form H_∞ controller for end-effector trajectory tracking within the space of unit dual quaternions;
- 2) Novel (kinematic) singularity-avoidance technique using H_∞ criteria.

Since the present paper builds upon our previous work [14], the list below provides the novelties with respect to that work:

- 1) The problem is reformulated to provide a geometrical meaning to noises and disturbances, making it easier to define the controllers' gains;
- 2) The controller has been extended to consider trajectory tracking (in [14] we solved only the regulation problem);
- 3) Proof of exponential convergence;

- 4) Kinematic singularities are regarded as a disturbance in the trajectory tracking, which enables us to easily extend the H_∞ controller to limit their influence upon the robot's behavior;
- 5) We perform realistic simulations in V-Rep.

II. PRELIMINARIES

This section provides for the reader basic concepts and a brief theoretical background regarding dual quaternion representation for rigid body motion.¹ We also address the description and the influence of different sources of exogenous disturbances and uncertainties which affect the accuracy of the system representation and, as a direct consequence, the control performance.

A. Dual quaternions applied to rigid motion representation

Let $\hat{i}, \hat{j}, \hat{k}$ be the three quaternionic units such that $\hat{i}^2 = \hat{j}^2 = \hat{k}^2 = \hat{i}\hat{j}\hat{k} = -1$. The algebra of quaternions [20] is generated by the basis elements $1, \hat{i}, \hat{j}$, and \hat{k} , which yields the set

$$\mathbb{H} \triangleq \left\{ \eta + \mu_1 \hat{i} + \mu_2 \hat{j} + \mu_3 \hat{k} : \eta, \mu_1, \mu_2, \mu_3 \in \mathbb{R} \right\}, \quad (1)$$

An element $\mathbf{h} \in \mathbb{H}$, where $\mathbf{h} = \eta + \mu_1 \hat{i} + \mu_2 \hat{j} + \mu_3 \hat{k}$, may be decomposed into a real component and an imaginary component

$$\text{Re}(\mathbf{h}) \triangleq \eta \quad \text{and} \quad \text{Im}(\mathbf{h}) \triangleq \mu_1 \hat{i} + \mu_2 \hat{j} + \mu_3 \hat{k},$$

such that $\mathbf{h} = \text{Re}(\mathbf{h}) + \text{Im}(\mathbf{h})$. Quaternion elements with real part equal to zero belong to the set of pure quaternions

$$\mathbb{H}_p \triangleq \{ \mathbf{h} \in \mathbb{H} : \text{Re}(\mathbf{h}) = 0 \}, \quad (2)$$

and are equivalent to vectors in \mathbb{R}^3 under the addition operation. Hence, both cross product and inner product are defined for elements of \mathbb{H}_p and are analogous to their counterparts in \mathbb{R}^3 . More specifically, given $\mathbf{u}, \mathbf{v} \in \mathbb{H}_p$, the inner product $\langle \mathbf{u}, \mathbf{v} \rangle$ and the cross product $\mathbf{u} \times \mathbf{v}$ are respectively defined as

$$\langle \mathbf{u}, \mathbf{v} \rangle \triangleq -\frac{\mathbf{u}\mathbf{v} + \mathbf{v}\mathbf{u}}{2} \quad \text{and} \quad \mathbf{u} \times \mathbf{v} \triangleq \frac{\mathbf{u}\mathbf{v} - \mathbf{v}\mathbf{u}}{2}. \quad (3)$$

The set of unit quaternions is defined as

$$\mathbb{S}^3 \triangleq \{ \mathbf{h} \in \mathbb{H} : \|\mathbf{h}\| = 1 \},$$

where $\|\mathbf{h}\| \triangleq \sqrt{\mathbf{h}\mathbf{h}^*} = \sqrt{\mathbf{h}^*\mathbf{h}}$ is the quaternion norm and $\mathbf{h}^* \triangleq \text{Re}(\mathbf{h}) - \text{Im}(\mathbf{h})$ is the conjugate of \mathbf{h} . The set \mathbb{S}^3 , together with the multiplication operation, forms the Lie group of unit quaternions, $\text{Spin}(3)$, whose identity element is 1 and the inverse of any element $\mathbf{h} \in \text{Spin}(3)$ is \mathbf{h}^* [21].

An arbitrary rotation angle $\phi \in \mathbb{R}$ around the rotation axis $\mathbf{n} \in \mathbb{H}_p \cap \mathbb{S}^3$, with $\mathbf{n} = n_x \hat{i} + n_y \hat{j} + n_z \hat{k}$, is represented by the unit quaternion $\mathbf{r} = \cos(\phi/2) + \sin(\phi/2)\mathbf{n}$ [22].

The complete rigid body motion, in which translation and rotation are coupled, is similarly described using dual quaternion algebra [21]. This algebra is constituted by the set

$$\mathcal{H} \triangleq \{ \mathbf{h} + \varepsilon \mathbf{h}' : \mathbf{h}, \mathbf{h}' \in \mathbb{H}, \varepsilon^2 = 0, \varepsilon \neq 0 \},$$

¹For more information on dual quaternion algebra, please see [7].

where ε is called dual unit. Given $\underline{h} \in \mathcal{H}$, with $\underline{h} = \mathbf{h} + \varepsilon\mathbf{h}'$, its norm is defined as $\|\underline{h}\| \triangleq \sqrt{\underline{h}\underline{h}^*} = \sqrt{\mathbf{h}^*\mathbf{h}}$ and the element $\underline{h}^* \triangleq \mathbf{h}^* + \varepsilon\mathbf{h}'^*$ is called the conjugate of \underline{h} . Under multiplication, the subset of *unit* dual quaternions

$$\underline{\mathcal{S}} \triangleq \{\underline{h} \in \mathcal{H} : \|\underline{h}\| = 1\}, \quad (4)$$

forms the Lie group $\text{Spin}(3) \times \mathbb{R}^3$, whose identity element is 1 and the group inverse of $\underline{x} \in \underline{\mathcal{S}}$ is \underline{x}^* [21].

An arbitrary rigid displacement defined by a translation $\mathbf{p} \in \mathbb{H}_p$ followed by a rotation $\mathbf{r} \in \mathbb{S}^3$ is represented in $\text{Spin}(3) \times \mathbb{R}^3$ by the element²

$$\underline{x} = \mathbf{r} + \varepsilon \frac{1}{2} \mathbf{p} \mathbf{r}. \quad (5)$$

The first order kinematic equation of a rigid body motion is described by

$$\dot{\underline{x}} = \frac{1}{2} \underline{\xi} \underline{x}, \quad (6)$$

where $\underline{\xi} = \boldsymbol{\omega} + \varepsilon(\dot{\mathbf{p}} + \mathbf{p} \times \boldsymbol{\omega})$ is the twist in the inertial frame and $\boldsymbol{\omega}, \dot{\mathbf{p}} \in \mathbb{H}_p$ are the angular and linear velocities, respectively. The twist belongs to the set \mathcal{H}_p of pure dual quaternions; that is, $\underline{\xi} \in \mathcal{H}_p$, where

$$\mathcal{H}_p \triangleq \{(\mathbf{h} + \varepsilon\mathbf{h}') \in \mathcal{H} : \text{Re}(\mathbf{h}) = \text{Re}(\mathbf{h}') = 0\}.$$

To simplify the notation throughout the paper, let us define the bijective mapping between \mathcal{H}_p and \mathbb{R}^6 by

$$\text{vec}_6 : \mathcal{H}_p \rightarrow \mathbb{R}^6, \quad (7)$$

such that, given $\underline{\xi} = (\xi_1\hat{i} + \xi_2\hat{j} + \xi_3\hat{k}) + \varepsilon(\xi_4\hat{i} + \xi_5\hat{j} + \xi_6\hat{k})$, then $\text{vec}_6 \underline{\xi} = [\xi_1 \ \dots \ \xi_6]^T$. The inverse mapping is defined by $\text{vec}_6 : \mathbb{R}^6 \rightarrow \mathcal{H}_p$.

Analogously, the bijective mapping $\mathbb{H}_p \rightarrow \mathbb{R}^3$ is given by the operator vec_3 , such that $\boldsymbol{\mu} = \mu_1\hat{i} + \mu_2\hat{j} + \mu_3\hat{k}$ yields $\text{vec}_3 \boldsymbol{\mu} = [\mu_1 \ \mu_2 \ \mu_3]^T$ and the inverse mapping is given by the operator vec_3 .

B. Forward Kinematics of Serial Manipulators using Dual Quaternions Algebra

A sequence of rigid motions can be represented by a sequence of unit dual quaternion multiplications, thus we can easily represent the end-effector pose of an n -joint serial manipulator by means of successive rigid transformations between its links. Hence, the rigid transformation from the robot's base to its end-effector pose—i.e., its forward kinematics—is described by $\underline{x}_N = \underline{x}_1^0 \underline{x}_2^1 \dots \underline{x}_n^{n-1}$, where $\underline{x}_{i+1}^i \in \text{Spin}(3) \times \mathbb{R}^3$ represents the rigid transformation between the extremities of links i and $i+1$ and \underline{x}_{i+1}^i is a function of joint configuration $q_{i+1} \in \mathbb{R}$; that is, $\underline{x}_{i+1}^i \triangleq \underline{x}_{i+1}^i(q_{i+1})$, therefore $\underline{x}_N \triangleq \underline{x}_N(\mathbf{q})$, where $\mathbf{q} = [q_1 \ \dots \ q_n]^T$.

The differential forward kinematics, as a consequence, defines the mapping between the joints velocities and the end-effector (generalized) velocity. Since the latter is given by

the time derivative of a unit dual quaternion, the first order differential kinematics is constrained by (6) such that

$$\begin{aligned} \dot{\underline{x}}_N &= \frac{1}{2} \underline{\xi}_N \underline{x}_N \\ &= \frac{1}{2} \sum_{i=1}^n \underline{\mathcal{J}}_i \dot{q}_i \underline{x}_N, \end{aligned} \quad (8)$$

where $\underline{x}_N = \underline{x}_N(\mathbf{q})$ is the pose obtained from the forward kinematics, and $\underline{\mathcal{J}}_i \in \mathcal{H}_p$ is given by [3]

$$\underline{\mathcal{J}}_i = 2\underline{x}_{i-1}^0 \frac{d\underline{x}_i^{i-1}}{dq_i} (\underline{x}_i^{i-1})^* \underline{x}_0^{i-1}.$$

It is important to note that the product $\underline{\mathcal{J}}_i \dot{q}_i$ corresponds to the twist of link i expressed in the base frame.

C. Influence of Uncertainties and Exogenous Disturbances

In most situations met in practice, the trajectory of the end-effector is likely to be influenced by different sources of exogenous disturbances and the manipulator's geometrical parameters may not be exactly accurate, resulting in an uncertain differential forward kinematics. To improve the kinematics accuracy and the control performance, the influence of those uncertainties and disturbances over the system must be explicitly regarded, as neglecting their influence would most likely lead to poor performance.

In this work, different sources of disturbances acting on a serial manipulator, classified as twist and pose uncertainties, are investigated, which leads to a more complete and accurate kinematics description. Twist uncertainties represent unmodeled twists describing multiple sources of exogenous disturbances that may influence the end-effector *velocity*, such as unmodeled time-varying uncertainties and forces acting on non-rigid manipulators. This way, the differential forward kinematics of a manipulator under the influence of a twist disturbance \underline{v}_w is given by³

$$\dot{\underline{x}}_N = \frac{1}{2} \sum_{i=1}^n \underline{\mathcal{J}}_i \dot{q}_i \underline{x}_N + \frac{1}{2} \underline{v}_w \underline{x}_N. \quad (9)$$

The second class of disturbances addressed herein, that is, the influence of uncertainties over the end-effector *pose*, also arises from unforeseen inaccuracies within model parameters and time-varying uncertainties, but also comprises inaccuracies in the location of the reference frame. Pose uncertainties depicts transformations in the forward kinematics model and, therefore, can be mapped to (8)–(9) as

$$\underline{x} = \underline{x}_N \underline{c}, \quad (10)$$

²Similarly, the rigid motion could also be represented by a rotation \mathbf{r} followed by a translation \mathbf{p} given the relation $\bar{\mathbf{p}} = \mathbf{r}^* \mathbf{p} \mathbf{r}$.

³It is important to note that (9) is well-posed (i.e., $\dot{\underline{x}}_N$ belongs to the tangent space of $\text{Spin}(3) \times \mathbb{R}^3$ at \underline{x}_N) as $\underline{v}_w \in \mathcal{H}_p$ is in the Lie algebra of $\text{Spin}(3) \times \mathbb{R}^3$.

where $\underline{c} \in \text{Spin}(3) \times \mathbb{R}^3$ and \underline{x} denotes the real pose of the disturbed end-effector. The time derivative of (10), taking into consideration (9), yields

$$\begin{aligned} \dot{\underline{x}} &= \dot{\underline{x}}_N \underline{c} + \underline{x}_N \dot{\underline{c}} = \frac{1}{2} \sum_{i=1}^n \mathcal{J}_i \dot{q}_i \underline{x}_N \underline{c} + \frac{1}{2} \underline{v}_w \underline{x}_N \underline{c} + \frac{1}{2} \underline{x}_N \underline{c} \underline{v}_c \\ &= \frac{1}{2} \sum_{i=1}^n \mathcal{J}_i \dot{q}_i \underline{x} + \frac{1}{2} \underline{v}_w \underline{x} + \frac{1}{2} \underline{x} \underline{v}_c, \end{aligned}$$

where $\underline{v}_c \in \mathcal{H}_p$ is the twist related to $\dot{\underline{c}}$, but expressed in the local frame; that is, $\dot{\underline{c}} = (1/2) \underline{c} \underline{v}_c$. Since the disturbance \underline{v}_c can be expressed in the inertial frame by means of the norm-preserving transformation $\underline{v}_c = \underline{x}^* \underline{v}_c \underline{x}$, then

$$\dot{\underline{x}} = \frac{1}{2} \sum_{i=1}^n \mathcal{J}_i \dot{q}_i \underline{x} + \frac{1}{2} \underline{v}_w \underline{x} + \frac{1}{2} \underline{v}_c \underline{x}. \quad (11)$$

Although both sources of uncertainties (\underline{v}_w and \underline{v}_c) could be grouped together into a single variable to ease the analysis (see Corollary 5), addressing them separately leads to more precise results and adds to the designer flexibility since it allows the consideration of different sources of disturbances.

D. Error Definition and Problem Statement

In this work, we are particularly interested in ensuring the end-effector tracks a desired trajectory while reducing the influence of uncertainties and disturbances upon the controlled pose. In other words, given a desired time-varying pose $\underline{x}_d(t) \in \text{Spin}(3) \times \mathbb{R}^3$, we seek to guarantee internal stability and tracking performance whilst reducing the noise-to-output influence over the end-effector trajectory.

To this aim, given a desired end-effector trajectory $\underline{x}_d(t)$ and the twist $\underline{\xi}_d \in \mathcal{H}_p$ satisfying the first order kinematic equation

$$\dot{\underline{x}}_d = \frac{1}{2} \underline{\xi}_d \underline{x}_d, \quad (12)$$

we define the spatial difference in $\text{Spin}(3) \times \mathbb{R}^3$ as

$$\underline{\tilde{x}} \triangleq \underline{x} \underline{x}_d^* = \tilde{r} + \varepsilon \frac{1}{2} \tilde{p} \tilde{r}, \quad (13)$$

where $\tilde{r} = r r_d^*$ denotes the orientation error in $\text{Spin}(3)$ given the desired orientation r_d , and $\tilde{p} = p - \tilde{r} p_d \tilde{r}^*$ denotes the translational error in \mathbb{H}_p given a desired position p_d .

Considering the rigid body kinematics subject to uncertainties and exogenous disturbances (11) with desired kinematics (12), the error kinematics is given by

$$\begin{aligned} \dot{\underline{\tilde{x}}} &= \dot{\underline{x}} \underline{x}_d^* + \underline{x} \dot{\underline{x}}_d^* \\ &= \frac{1}{2} \left(\sum_{i=1}^n \mathcal{J}_i \dot{q}_i \underline{x} + \underline{v}_w \underline{x} + \underline{v}_c \underline{x} \right) \underline{x}_d^* + \frac{1}{2} \underline{x} \underline{x}_d^* \underline{\xi}_d^* \\ &= \frac{1}{2} \left(\sum_{i=1}^n \mathcal{J}_i \dot{q}_i + \underline{v}_w + \underline{v}_c \right) \underline{\tilde{x}} - \frac{1}{2} \underline{\tilde{x}} \underline{\xi}_d. \end{aligned} \quad (14)$$

From the spatial difference (13), we define a right invariant dual quaternion error function⁴

$$\underline{\tilde{z}} \triangleq 1 - \underline{\tilde{x}} = \tilde{z} + \varepsilon \tilde{z}' \quad (15)$$

with dynamics described by $\dot{\underline{\tilde{z}}} = -\underline{\tilde{x}} \underline{\tilde{z}}$. Therefore, $\underline{\tilde{z}} \rightarrow 0$ implies $\underline{\tilde{x}} \rightarrow 1$, which implies $\underline{x} \rightarrow \underline{x}_d$.

To address H_∞ performance, let us first introduce the gain that defines the H_∞ norm that arises from the induced norm of the map $\underline{v} \mapsto \underline{z}$, where $\underline{v}, \underline{z} \in L_2[0, \infty)^5$ represent a generic noise signal and the desired output state, respectively [23]. This way, the H_∞ gain represents the supremum of the noise amplification upon the system output; that is,

$$\sup \left\{ \frac{\int_0^\infty \|\underline{z}(t)\|^2 dt}{\int_0^\infty \|\underline{v}(t)\|^2 dt}, \underline{v}(t) \in L_2(0, \infty) \right\}, \quad (16)$$

which is the worst-case influence of the noise \underline{v} over the controlled output \underline{z} . The main advantage of the H_∞ norm is the needlessness for assumptions regarding the statistics of the uncertainties and noises—although this information, if available, can improve analysis [24]. This is particularly useful for the space of rigid body transformations as probability density functions are, in general, hard to characterize for such non-Euclidean spaces.

Since a direct minimization of (16) may not be tractable, we introduce a variable γ that upper bounds the induced norm; that is,

$$\int_0^\infty \|\underline{z}(t)\|^2 dt \leq \gamma^2 \int_0^\infty \|\underline{v}(t)\|^2 dt.$$

The smaller is the value of the noise-to-output upper bound γ , the smaller is the influence of \underline{v} over \underline{z} . Hence, the reduction of the index γ provides a way of reducing the disturbance influence on the output \underline{z} . Furthermore, to address the detrimental influence of the uncertainties and disturbances in system (14), we assume that $\underline{v}_w, \underline{v}'_w, \underline{v}_c, \underline{v}'_c \in L_2[0, \infty)$.

For the H_∞ control performance, we address as variable of interest the orientation and position errors from (13) and (15), defined respectively as

$$\begin{aligned} \mathcal{O}(\underline{\tilde{z}}) &\triangleq \text{Im}(\underline{\tilde{z}}), \\ \mathcal{T}(\underline{\tilde{z}}) &\triangleq \tilde{p}. \end{aligned} \quad (17)$$

Remark 1. Both attitude and position error outputs (i.e., $\mathcal{O}(\underline{\tilde{z}})$ and $\mathcal{T}(\underline{\tilde{z}})$) can be easily extracted from $\underline{\tilde{z}}$. The former is the imaginary component of the attitude error ($\underline{\tilde{z}} = \text{Re}(\underline{\tilde{z}}) + \text{Im}(\underline{\tilde{z}})$) from (15), which is given explicitly by $\text{Im}(\underline{\tilde{z}}) = -\sin(\tilde{\phi}/2) \tilde{n}$, where $\tilde{\phi}$ and \tilde{n} are respectively the rotation angle and rotation axis from \tilde{r} in (13). The position error is extracted from (13) and (15) using $\tilde{p} = -2\tilde{z}'(1-\tilde{z}^*)$.

In this context, the following definition describes the robust performance (in the H_∞ sense) in terms of the dual quaternion error (15) and the disturbances \underline{v}_w and \underline{v}_c .

Definition 2. For prescribed positive scalars $\gamma_{o1}, \gamma_{o2}, \gamma_{T1}, \gamma_{T2}$, the robust control performance is achieved, in the H_∞ sense, if the following hold [23]

- (1) The error (15) is exponentially stable for $\underline{v}_w = \underline{v}_c = 0$;
- (2) Under the assumption of zero initial conditions, the disturbances' influence upon the attitude and translation errors is

⁴In order to prevent the unwinding phenomenon, see Remark 7.

⁵ L_2 is the Hilbert space of all square-integrable functions.

attenuated below a desired level; that is, $\forall (\mathbf{v}_w, \mathbf{v}_c, \mathbf{v}'_w, \mathbf{v}'_c) \in L_2(0, \infty)$

$$\begin{aligned} \int_0^\infty \|\mathcal{O}(\tilde{\mathbf{z}}(t))\|^2 dt &\leq \gamma_{\sigma_1}^2 \int_0^\infty \|\mathbf{v}_w(t)\|^2 dt + \gamma_{\sigma_2}^2 \int_0^\infty \|\mathbf{v}_c(t)\|^2 dt, \\ \int_0^\infty \|\mathcal{S}(\tilde{\mathbf{z}}(t))\|^2 dt &\leq \gamma_{\tau_1}^2 \int_0^\infty \|\mathbf{v}'_w(t)\|^2 dt + \gamma_{\tau_2}^2 \int_0^\infty \|\mathbf{v}'_c(t)\|^2 dt. \end{aligned} \quad (18)$$

III. H_∞ CONTROL STRATEGIES

As discussed in Section II, the impact of different sources of uncertainties and disturbances over the system kinematics must be explicitly regarded, and the controller must be designed in accordance to their influence, as neglecting their effects jeopardizes the overall stability.

In this sense, this section presents a new control strategy that ensures H_∞ performance for both set-point control and tracking problems without decoupling the rotational and translational dynamics. Since traditional H_∞ theory is unable to deal with multiplicative noises, the proposed analysis exploits the dual quaternion algebra properties to solve the H_∞ problem while taking into account both additive and multiplicative disturbances.

A. H_∞ set-point control

First, let us consider an H_∞ set point control based on (14). In this case, $\underline{\xi}_d = 0$, thus

$$\dot{\tilde{\mathbf{x}}} = \frac{1}{2} \left(\sum_{i=1}^n \mathbf{J}_i \dot{q}_i + \mathbf{v}_w + \mathbf{v}_c \right) \tilde{\mathbf{x}}. \quad (19)$$

Furthermore, using the inverse mapping of (7) in (19) yields

$$\dot{\tilde{\mathbf{x}}} = \frac{1}{2} (\text{vec}_6(\mathbf{J}\dot{\mathbf{q}}) + \mathbf{v}_w + \mathbf{v}_c) \tilde{\mathbf{x}}, \quad (20)$$

where $\mathbf{q} = [q_1 \ \cdots \ q_n]^T$ is the vector of joint variables and $\mathbf{J} = [\text{vec}_6 \mathbf{J}_1 \ \cdots \ \text{vec}_6 \mathbf{J}_n]$ is the (twist) Jacobian matrix that maps the joints velocities $\dot{\mathbf{q}}$ to the (undisturbed) twist $\text{vec}_6 \underline{\xi}_N$ of the end-effector.

To solve the problem of robust exponential stabilization of the dual quaternion error function (20), we propose the following controller

$$\dot{\mathbf{q}} = \mathbf{J}^+ \begin{bmatrix} \kappa_\sigma \text{vec}_3 \mathcal{O}(\tilde{\mathbf{z}}) \\ -\kappa_\tau \text{vec}_3 \mathcal{S}(\tilde{\mathbf{z}}) \end{bmatrix}, \quad (21)$$

where $\kappa_\sigma, \kappa_\tau \in (0, \infty)$ denotes the scalar control gains, \mathbf{J}^+ is the Moore-Penrose pseudo-inverse of \mathbf{J} , and $\mathcal{O}(\tilde{\mathbf{z}})$ and $\mathcal{S}(\tilde{\mathbf{z}})$ are given by (17).

Theorem 3 (H_∞ Setpoint Control). *For prescribed positive scalars $\gamma_{\sigma_1}, \gamma_{\sigma_2}, \gamma_{\tau_1}, \gamma_{\tau_2}$, the closed-loop system (20)–(21) with $\kappa_\sigma = (\gamma_{\sigma_1}^{-2} + \gamma_{\sigma_2}^{-2})^{1/2}$ and $\kappa_\tau = (\gamma_{\tau_1}^{-2} + \gamma_{\tau_2}^{-2})^{1/2}$ achieves exponential stability with H_∞ disturbance attenuation in the sense of Definition 2 with minimum control effort.*

Proof: (Exponential stability) To study the stability of the closed loop system, let us regard the following Lyapunov candidate function

$$V(t, \tilde{\mathbf{z}}) = V_1(t, \tilde{\mathbf{z}}) + V_2(t, \tilde{\mathbf{z}}'), \quad (22)$$

where $V_1(t, \tilde{\mathbf{z}}) \triangleq \alpha_1 \|\tilde{\mathbf{z}}(t)\|^2$ and $V_2(t, \tilde{\mathbf{z}}') \triangleq \alpha_2 \|\tilde{\mathbf{z}}'(t)\|^2$ with given positive scalars α_1 and α_2 . The time-derivative of (22), considering the control input (21) (see Appendix A) in the absence of disturbances (i.e., $\mathbf{v}_w = \mathbf{v}_c = 0$) yields

$$\dot{V}_1(t, \tilde{\mathbf{z}}) \leq -\frac{\kappa_\sigma}{2} \alpha_1 \|\tilde{\mathbf{z}}(t)\|^2,$$

$$\dot{V}_2(t, \tilde{\mathbf{z}}') = -2\kappa_\tau \alpha_2 \|\tilde{\mathbf{z}}'(t)\|^2.$$

Hence, the closed-loop system (20) with the proposed controller (21), in the absence of disturbances, satisfy the following inequalities

$$\dot{V}(t, \tilde{\mathbf{z}}) \leq -\frac{\kappa_\sigma}{2} \alpha_1 \|\tilde{\mathbf{z}}(t)\|^2 - 2\kappa_\tau \alpha_2 \|\tilde{\mathbf{z}}'(t)\|^2 \quad (23)$$

$$\leq -\min \left\{ \frac{\kappa_\sigma}{2}, 2\kappa_\tau \right\} V(t, \tilde{\mathbf{z}}) \leq 0,$$

which implies, by the Comparison Lemma [25, p. 85], that the closed-loop system is exponentially stable; that is,

$$\dot{V}(t, \tilde{\mathbf{z}}) \leq V(t_0, \tilde{\mathbf{z}}(t_0)) \exp \left(-\min \left\{ \frac{\kappa_\sigma}{2}, 2\kappa_\tau \right\} (t - t_0) \right).$$

This way, Condition 1 in Definition 2 is satisfied for positive real scalars κ_σ and κ_τ . In addition, by using the Comparison Lemma together with (44) and (45), it is possible to show that both individual attitude and translation dynamics achieve exponential stability in the absence of disturbances, that is,

$$\|\tilde{\mathbf{z}}(t)\|^2 \leq \|\tilde{\mathbf{z}}(t_0)\|^2 \exp \left(-\frac{1}{2} \kappa_\sigma (t - t_0) \right),$$

$$\|\tilde{\mathbf{z}}'(t)\|^2 = \|\tilde{\mathbf{z}}'(t_0)\|^2 \exp(-2\kappa_\tau (t - t_0)).$$

(Disturbance attenuation) In order to verify Condition 2 in Definition 2, now we explicitly consider the influence of uncertainties and disturbances over the closed-loop system. As a consequence, the Lyapunov derivative yields (see (46) in Appendix A)

$$\begin{aligned} \dot{V}(t, \tilde{\mathbf{z}}) &= \overbrace{-\alpha_1 \langle \mathcal{O}(\tilde{\mathbf{z}}), \kappa_\sigma \mathcal{O}(\tilde{\mathbf{z}}) + \mathbf{v}_w + \mathbf{v}_c \rangle}^{V_1(t, \tilde{\mathbf{z}})} \\ &\quad - \underbrace{\frac{\alpha_2}{2} \langle \mathcal{S}(\tilde{\mathbf{z}}), \kappa_\tau \mathcal{S}(\tilde{\mathbf{z}}) - \mathbf{v}'_w - \mathbf{v}'_c \rangle}_{V_2(t, \tilde{\mathbf{z}})}. \end{aligned} \quad (24)$$

Defining $V_{\gamma_\sigma} \triangleq \|\mathcal{O}(\tilde{\mathbf{z}})\|^2 - \gamma_{\sigma_1}^2 \|\mathbf{v}_w\|^2 - \gamma_{\sigma_2}^2 \|\mathbf{v}_c\|^2$ and $V_{\gamma_\tau} \triangleq \|\mathcal{S}(\tilde{\mathbf{z}})\|^2 - \gamma_{\tau_1}^2 \|\mathbf{v}'_w\|^2 - \gamma_{\tau_2}^2 \|\mathbf{v}'_c\|^2$, Condition 2 is fulfilled if, for all $t \in [0, \infty)$, the following inequalities hold

$$\dot{V}_1(t, \tilde{\mathbf{z}}) + V_{\gamma_\sigma} \leq 0, \quad (25)$$

$$\dot{V}_2(t, \tilde{\mathbf{z}}) + V_{\gamma_\tau} \leq 0. \quad (26)$$

This is due to the fact that, under zero initial conditions (i.e., $V(0, \tilde{\mathbf{z}}(0)) = 0$), we have

$$\int_0^\infty V_{\gamma_\sigma} dt \leq -\int_0^\infty \dot{V}_1(t, \tilde{\mathbf{z}}) dt = V_1(0, \tilde{\mathbf{z}}) - \lim_{t \rightarrow \infty} V_1(t, \tilde{\mathbf{z}}) \leq 0,$$

where the last inequality holds because $V_1(0, \tilde{\mathbf{z}}(0)) = 0$ and $V_1(t, \tilde{\mathbf{z}}) \geq 0, \forall t$, which implies the first inequality of Condition 2 in Definition 2. The same reasoning applies to (26).

In order to satisfy (25), we first use the definition of inner product as in (3) to rewrite (25) as⁶

$$\begin{bmatrix} \mathcal{O}(\tilde{\mathbf{z}}) \\ \mathbf{v}_w \\ \mathbf{v}_c \end{bmatrix}^* \underbrace{\begin{bmatrix} -(\alpha_1 \kappa_\circ - 1) & -\alpha_{1/2} & -\alpha_{1/2} \\ -\alpha_{1/2} & -\gamma_{\circ 1}^2 & 0 \\ -\alpha_{1/2} & 0 & -\gamma_{\circ 2}^2 \end{bmatrix}}_M \begin{bmatrix} \mathcal{O}(\tilde{\mathbf{z}}) \\ \mathbf{v}_w \\ \mathbf{v}_c \end{bmatrix} \leq 0. \quad (27)$$

Since $M \leq 0$ implies (27),⁷ by using Schur complements it is possible to show that $M \leq 0$ if and only if

$$\kappa_\circ \geq \frac{1}{\alpha_1} + \frac{\alpha_1}{4} (\gamma_{\circ 1}^{-2} + \gamma_{\circ 2}^{-2}). \quad (28)$$

We repeat the same procedure for (26) to obtain

$$\kappa_\tau \geq \frac{2}{\alpha_2} + \frac{\alpha_2}{8} (\gamma_{\tau 1}^{-2} + \gamma_{\tau 2}^{-2}). \quad (29)$$

(Minimum control effort) Since there exist an infinite number of solutions for α_1 and α_2 that satisfy (28) and (29), we seek $\alpha_{1\text{opt}}$ and $\alpha_{2\text{opt}}$ that minimize the positive control gains κ_\circ and κ_τ . By letting $f(\alpha_1) \triangleq \alpha_1^{-1} + (1/4)\alpha_1\gamma_\circ$ and $g(\alpha_2) \triangleq 2\alpha_2^{-1} + (1/8)\alpha_2\gamma_\tau$, where $\gamma_\circ \triangleq \gamma_{\circ 1}^{-2} + \gamma_{\circ 2}^{-2}$ and $\gamma_\tau \triangleq \gamma_{\tau 1}^{-2} + \gamma_{\tau 2}^{-2}$, we minimize $f(\alpha_1)$ and $g(\alpha_2)$ with respect to α_1 and α_2 , respectively, to obtain $\alpha_{1\text{opt}} = 2\gamma_\circ^{-1/2}$ and $\alpha_{2\text{opt}} = 4\gamma_\tau^{-1/2}$. Therefore, the minimum values for the control gains κ_\circ and κ_τ that satisfy (28) and (29) are

$$\begin{aligned} \kappa_\circ &= f(\alpha_{1\text{opt}}) = (\gamma_{\circ 1}^{-2} + \gamma_{\circ 2}^{-2})^{1/2}, \\ \kappa_\tau &= g(\alpha_{2\text{opt}}) = (\gamma_{\tau 1}^{-2} + \gamma_{\tau 2}^{-2})^{1/2}. \end{aligned}$$

The set-point control scheme provided by Theorem 3 is a straightforward solution to the H_∞ control of manipulators using dual quaternion representation. Indeed, the resulting controller gains are given by a closed-form expression and solely depends on the prescribed scalars, $\gamma_{\circ 1}, \gamma_{\circ 2}, \gamma_{\tau 1}, \gamma_{\tau 2}$, which are related to the desired disturbance attenuation. Furthermore, the resulting control scheme is optimal in the sense of minimizing the gain values, which in turn reduces the control effort required to exponentially stabilize the end effector while attenuating the exogenous disturbances. Furthermore, gain values greater than the optimal ones result in a faster convergence rate, while still satisfying the H_∞ performance, at the expense of a larger control effort.

B. H_∞ tracking control

Several applications require convergence to time-varying reference trajectories. The desired end-effector trajectory over time is described by the first order kinematic equation (12) with corresponding error differential kinematics given by (14).

Similarly to the previous section, we use the mapping (7) to rewrite (14) as

$$\dot{\tilde{\mathbf{x}}} = \frac{1}{2} (\text{vec}_6(\mathbf{J}\dot{\mathbf{q}}) + \mathbf{v}_w + \mathbf{v}_c) \tilde{\mathbf{x}} - \frac{1}{2} \tilde{\mathbf{x}} \underline{\xi}_d \tilde{\mathbf{x}}, \quad (30)$$

⁶Notice that Γ^* is the (quaternion) conjugate transpose of a matrix $\Gamma \in \mathbb{H}^{m \times n}$, which is defined analogously to the conjugate transpose of complex numbers.

⁷Given a symmetric matrix $M \in \mathbb{R}^{n \times n}$, if $\mathbf{u}^T M \mathbf{u} \leq 0, \forall \mathbf{u} \in \mathbb{R}^n$, then $\Gamma^* M \Gamma \leq 0, \forall \Gamma \in \mathbb{H}^n$.

where $\mathbf{q} = [q_1 \ \cdots \ q_n]^T$ is the measured vector of joint variables and $\mathbf{J} = [\text{vec}_6 \mathbf{J}_1 \ \cdots \ \text{vec}_6 \mathbf{J}_n]$ is the analytical (twist) Jacobian.

From Definition 2 and Theorem 3, we state a solution for the H_∞ tracking control problem as follows.

Theorem 4 (H_∞ Tracking Control). *For prescribed positive scalars $\gamma_{\circ 1}, \gamma_{\circ 2}, \gamma_{\tau 1}, \gamma_{\tau 2}$, the task-space controller yielding joints' velocity inputs*

$$\dot{\mathbf{q}} = \mathbf{J}^+ \left(\begin{bmatrix} \kappa_\circ \text{vec}_3 \mathcal{O}(\tilde{\mathbf{z}}) \\ -\kappa_\tau \text{vec}_3 \mathcal{F}(\tilde{\mathbf{z}}) \end{bmatrix} + \text{vec}_6 \left(\tilde{\mathbf{x}} \underline{\xi}_d \tilde{\mathbf{x}}^* \right) \right), \quad (31)$$

with $\kappa_\circ = (\gamma_{\circ 1}^{-2} + \gamma_{\circ 2}^{-2})^{1/2}$ and $\kappa_\tau = (\gamma_{\tau 1}^{-2} + \gamma_{\tau 2}^{-2})^{1/2}$, ensures exponential H_∞ tracking performance with disturbance attenuation in the sense of Definition 2 with minimum control effort for the closed-loop system (30)–(31).

Proof: Replacing (31) in (30) we obtain⁸

$$\begin{aligned} \dot{\tilde{\mathbf{x}}} &= \frac{1}{2} (\text{vec}_6(\mathbf{J}\dot{\mathbf{q}}) + \mathbf{v}_w + \mathbf{v}_c) \tilde{\mathbf{x}} - \frac{1}{2} \tilde{\mathbf{x}} \underline{\xi}_d \tilde{\mathbf{x}} \\ &= \frac{1}{2} (\text{vec}_6(\mathbf{J}\dot{\mathbf{q}}) + \mathbf{v}_w + \mathbf{v}_c) \tilde{\mathbf{x}}, \end{aligned} \quad (32)$$

where $\dot{\mathbf{q}} = \mathbf{J}^+ \left[\kappa_\circ (\text{vec}_3 \mathcal{O}(\tilde{\mathbf{z}}))^T \quad -\kappa_\tau (\text{vec}_3 \mathcal{F}(\tilde{\mathbf{z}}))^T \right]^T$. Since (32) is the same closed-loop dynamics obtained from (20) under control law (21), the rest of the proof follows exactly the same steps from Theorem 3. ■

From Theorems 3 and 4, it is also interesting to consider particular cases where either it is difficult to decouple both sources of uncertainties or the designer explicitly sets the performance to be the same, that is, $\gamma_\tau \triangleq \gamma_{\tau 1} = \gamma_{\tau 2}$ and $\gamma_\circ \triangleq \gamma_{\circ 1} = \gamma_{\circ 2}$.

Corollary 5. *For prescribed positive scalars $\gamma_\circ, \gamma_\tau$, the closed-loop system (30) with task-space controller yielding joint velocity inputs defined in (31) and $\kappa_\circ = \sqrt{2}\gamma_\circ^{-1}$ and $\kappa_\tau = \sqrt{2}\gamma_\tau^{-1}$ achieves exponential H_∞ tracking performance with disturbance attenuation in the sense of Definition 2 with minimum control effort.*

Proof: The proof is identical to the one of Theorem 4 with $\gamma_\tau \triangleq \gamma_{\tau 1} = \gamma_{\tau 2}$ and $\gamma_\circ \triangleq \gamma_{\circ 1} = \gamma_{\circ 2}$. ■

C. H_∞ singularity-avoidance control

The controllers presented in previous sections rely on the assumption that the pseudo-inverse of the Jacobian matrix \mathbf{J} is well-conditioned at any given configuration; that is, the robot is never close to singular configurations. Because the Jacobian matrix becomes ill-conditioned near singularities, the control laws (21) and (31) may generate arbitrarily large input signals if the robot is sufficiently close to a singular configuration, which in turn may result in unstable behavior or poor performance [26].

⁸Eq. (32) holds even if the desired trajectory $\underline{\xi}_d$ is not feasible, that is, $\mathbf{J}\mathbf{J}^+ \text{vec}_6 \left(\tilde{\mathbf{x}} \underline{\xi}_d \tilde{\mathbf{x}}^* \right) \neq \text{vec}_6 \left(\tilde{\mathbf{x}} \underline{\xi}_d \tilde{\mathbf{x}}^* \right)$. In that case, let $\mathbf{s} \triangleq \text{vec}_6 \left(\tilde{\mathbf{x}} \underline{\xi}_d \tilde{\mathbf{x}}^* \right)$ then $\text{vec}_6(\mathbf{J}\mathbf{J}^+ \mathbf{s}) = \text{vec}_6(\mathbf{s}) + \underline{\mathbf{v}}_s$, where $\underline{\mathbf{v}}_s$ is just another source of disturbance to be added into $\underline{\mathbf{v}}_w$.

Redundant manipulators may recover from escapable singularities (i.e., singularities that can be avoided by changing the robot configuration) by using optimization techniques over some manipulability function that quantifies the proximity to a singular configuration. Usually, the control signals generated by the optimization process are projected onto the nullspace of the Jacobian matrix [27]–[29] to ensure that the end-effector trajectory is not influenced by the strategy of singularity avoidance.

In the case of non-redundant manipulators (where there is only a finite number of feasible configurations for each pose in task-space) or inescapable singularities (where the end-effector trajectory must inevitably be modified in order to escape from singularities), singularity avoidance can only be achieved with detriment to the planned task trajectory. In those cases, most techniques either rely on offline replanning the trajectory based on the knowledge of all singularities [30], [31], which are usually restricted to particular robots as singularities are hard to obtain for arbitrary manipulators, or on online modification of the Jacobian matrix based on the proximity to singular configurations [16]–[19].

Classic solutions to the online modification of the Jacobian matrix introduce a damping factor to the Jacobian least-square inverse [16] and some of them provide insights on the influence of the damping factor over the task trajectory [17], [18]. However, none of them defines an explicit trade-off metric between singularity avoidance and trajectory tracking *while* formally ensuring closed-loop stability in task-space. In this sense, we define a new strategy of singularity avoidance that exploits the H_∞ norm and performance criterion, given by Definition 2, to address the problem of inescapable singularities while providing formal stability and performance guarantees such as the worst-case influence of the singularity upon trajectory tracking.

To this end, at the vicinity of singular configurations, we introduce an induced exogenous twist acting upon the dual quaternion spatial difference, (20) and (30), such that the control inputs required by unachievable components of the task velocity are properly attenuated. The strategy is similar to the one proposed in [19] for Euclidean manifolds. Nonetheless, in contrast to [19], in our work the influence of the induced signal upon the trajectory error is bounded, and both the robust closed-loop stability and performance of the end-effector trajectory tracking are ensured.

It is reasonable to design the induced exogenous disturbance as a function of a given manipulability function. Given the robot Jacobian matrix \mathbf{J} , a common choice for the manipulability function is $\mathcal{M}(\mathbf{J}) = \sigma_1 \cdots \sigma_m$, which is the product of the singular values $\sigma_1, \dots, \sigma_m$ of \mathbf{J} [32]. When the Jacobian matrix is square, that manipulability function is equivalent to $\mathcal{M}(\mathbf{J}) = |\det \mathbf{J}|$, but it lacks monotonicity and, consequently, poorly quantifies the proximity to singularities. For instance, given $\mathbf{A} = \text{diag}(100, 0.02)$ and $\mathbf{B} = \mathbf{I}$, it is clear that \mathbf{A} is closer to the singularity, but $\mathcal{M}(\mathbf{A}) > \mathcal{M}(\mathbf{B})$.

In this context, we propose a more appropriate bounded function that increases monotonically as the singular values of the Jacobian matrix tend to zero. More specifically, consider the singular value decomposition of the Jacobian $\mathbf{J} \in \mathbb{R}^{6 \times n}$

with n being the number of joints,

$$\mathbf{J} = \mathbf{M} \begin{bmatrix} \mathbf{S} & \mathbf{0}_{s \times (n-s)} \\ \mathbf{0}_{(6-s) \times s} & \mathbf{0}_{(6-s) \times (n-s)} \end{bmatrix} \mathbf{N}^T = \sum_{i=1}^s \sigma_i \mathbf{m}_i \mathbf{n}_i^T, \quad (33)$$

where $[\mathbf{m}_1 \cdots \mathbf{m}_6] = \mathbf{M} \in \text{O}(6)$ and $[\mathbf{n}_1 \cdots \mathbf{n}_n] = \mathbf{N} \in \text{O}(n)$ are orthogonal matrices; $\mathbf{S} = \text{diag}(\sigma_1, \dots, \sigma_s)$, with $\sigma_1 \geq \sigma_2 \cdots \geq \sigma_s \geq 0$, is a diagonal matrix with entries corresponding to the singular values of \mathbf{J} ; and $s \leq 6$ is the rank of \mathbf{J} .

Given a particular singular value $\sigma_i \triangleq \sigma_i(\mathbf{J})$, $i \in \{1, \dots, s\}$, we define a function $f_\sigma : [0, \infty) \rightarrow [0, \sigma_{\text{far}}]$ such that

$$f_\sigma(\sigma_i) \triangleq \begin{cases} \sigma_{\text{far}} \left(1 - \frac{\sigma_i}{\sigma_{\text{region}}}\right), & \text{if } \sigma_i \leq \sigma_{\text{region}}, \\ 0, & \text{otherwise,} \end{cases} \quad (34)$$

where $\sigma_{\text{far}} > 1$ is an upper bound for f_σ and σ_{region} defines the boundary of the singular region. We also define the set

$$\text{sing}(\mathbf{J}) \triangleq \{\sigma \in \{\sigma_1, \dots, \sigma_s\} : \sigma \leq \sigma_{\text{region}}\},$$

whose elements correspond to the singular values that are in the vicinity of a singularity.

Singular values inside $\text{sing}(\mathbf{J})$ may result in arbitrarily large joints velocities if (21) or (31) is used to generate the control inputs. In order to clearly see this fact, let us recall that the pseudo-inverse of $\mathbf{J} \in \mathbb{R}^{6 \times n}$ is given by

$$\mathbf{J}^+ = \mathbf{N} \begin{bmatrix} \mathbf{S}^{-1} & \mathbf{0}_{s \times (6-s)} \\ \mathbf{0}_{(n-s) \times s} & \mathbf{0}_{(n-s) \times (6-s)} \end{bmatrix} \mathbf{M}^T = \sum_{i=1}^s \frac{1}{\sigma_i} \mathbf{n}_i \mathbf{m}_i^T, \quad (35)$$

where $\mathbf{N} = [\mathbf{n}_1 \cdots \mathbf{n}_n]$ and $\mathbf{M} = [\mathbf{m}_1 \cdots \mathbf{m}_6]$. Thus, since $\sigma_i \in \text{sing}(\mathbf{J})$ can be arbitrarily small, σ_i^{-1} can be arbitrarily large, which may result in arbitrarily large velocities in the direction of the corresponding vector \mathbf{n}_i .

Since negative effects in the neighborhood of singularities have a direct relation with the control inputs, we define an auxiliary control input that counteracts such effects and yields a limited disturbance to the end-effector trajectory. As a result, under reasonable initial conditions we can use Theorems 3, 4, or Corollary 5 to bound the influence of the singularity over the end-effector trajectory while ensuring stability properties. This is formally stated in the next theorem.

Theorem 6 (H_∞ Singularity-Robust Tracking Control). *Consider the control input*

$$\dot{\mathbf{q}} = \underbrace{\mathbf{P}_\sigma \mathbf{J}^+ \left(\begin{bmatrix} \kappa_\sigma \text{vec}_3 \mathcal{O}(\tilde{\mathbf{z}}) \\ -\kappa_\tau \text{vec}_3 \mathcal{I}(\tilde{\mathbf{z}}) \end{bmatrix} + \text{vec}_6 \left(\tilde{\mathbf{x}} \tilde{\boldsymbol{\xi}}_d \tilde{\mathbf{x}}^* \right) \right)}_{\dot{\mathbf{q}}_N} \quad (36)$$

with

$$\mathbf{P}_\sigma \triangleq \left(\mathbf{I} - \kappa_s \mathbf{N}_{\bar{s}} \mathbf{N}_{\bar{s}}^T \right),$$

where $\kappa_s \triangleq \min(f_\sigma(\sigma_{\min}), 1)$, in which f_σ is given by (34), σ_{\min} is the minimum singular value in $\text{sing}(\mathbf{J})$, the submatrix $\mathbf{N}_{\bar{s}} = [\mathbf{n}_{s-\bar{s}+1} \cdots \mathbf{n}_s] \in \mathbb{R}^{n \times \bar{s}}$ of \mathbf{N} contains the left (output) singular vectors of \mathbf{J}^+ corresponding to the singular values inside the singular region, and \bar{s} is the number of elements in $\text{sing}(\mathbf{J})$. The following statements are true:

1) *The auxiliary control input*

$$\dot{\mathbf{q}}_S = -\kappa_s \mathbf{N}_{\bar{s}} \mathbf{N}_{\bar{s}}^T \dot{\mathbf{q}}_N \quad (37)$$

acts only in the direction of the singular values that are inside the singular region;

2) *The disturbance $\underline{\mathbf{v}}_s \triangleq \text{vec}_6(\mathbf{J}\dot{\mathbf{q}}_S)$ induced by the proximity to singularities is bounded and there exists a lower bound for the minimum singular value of \mathbf{J} , namely $\sigma_{\min} \geq \sigma_{\text{region}}(1 - \sigma_{\text{far}}^{-1})$, $\forall t \geq 0$;*

3) *For prescribed positive scalars $\gamma_{\mathcal{O}}$, $\gamma_{\mathcal{T}}$, σ_{far} , and σ_{region} , and assuming that both $\mathbf{q}(0)$ and the stable point are not inside a singular region, the task-space controller (36) with $\kappa_{\mathcal{O}} = \sqrt{2}\gamma_{\mathcal{O}}^{-1}$ and $\kappa_{\mathcal{T}} = \sqrt{2}\gamma_{\mathcal{T}}^{-1}$, ensures exponential H_{∞} singularity-robust tracking performance with disturbance attenuation in the sense of Definition 2 with minimum control effort for the closed-loop system (30),(36).*

Proof: (Statement 1) Since $\dot{\mathbf{q}}_S \in \text{span}(\mathbf{n}_{s-\bar{s}+1}, \dots, \mathbf{n}_s)$, it is clear that the auxiliary control input acts only along the left singular vectors of \mathbf{J}^+ corresponding to the \bar{s} singular values of \mathbf{J} that are inside the singular region. In order to show that those inputs counteracts the components related to the singular region, let us define

$$\mathbf{\Gamma} \triangleq \left(\begin{bmatrix} \kappa_{\mathcal{O}} \text{vec}_3 \mathcal{O}(\underline{\mathbf{z}}) \\ -\kappa_{\mathcal{T}} \text{vec}_3 \mathcal{T}(\underline{\mathbf{z}}) \end{bmatrix} + \text{vec}_6(\underline{\mathbf{x}}_{\underline{\mathbf{d}}} \underline{\mathbf{x}}^*) \right)$$

and use (35) to obtain

$$\dot{\mathbf{q}}_N = \mathbf{J}^+ \mathbf{\Gamma} = \sum_{i=1}^s \frac{1}{\sigma_i} \mathbf{n}_i \mathbf{m}_i^T \mathbf{\Gamma}.$$

As $\mathbf{n}_i^T \mathbf{n}_j = 0 \forall i \neq j$, and $\mathbf{n}_i^T \mathbf{n}_j = 1$ when $i = j$, we obtain

$$\begin{aligned} \dot{\mathbf{q}}_S &= -\kappa_s \mathbf{N}_{\bar{s}} \mathbf{N}_{\bar{s}}^T \dot{\mathbf{q}}_N \\ &= -\kappa_s \left(\sum_{i=s-\bar{s}+1}^s \mathbf{n}_i \mathbf{n}_i^T \right) \left(\sum_{i=1}^{s-\bar{s}} \frac{1}{\sigma_i} \mathbf{n}_i \mathbf{m}_i^T + \sum_{i=s-\bar{s}+1}^s \frac{1}{\sigma_i} \mathbf{n}_i \mathbf{m}_i^T \right) \mathbf{\Gamma} \\ &= -\kappa_s \sum_{i=s-\bar{s}+1}^s \frac{1}{\sigma_i} \mathbf{n}_i \mathbf{m}_i^T \mathbf{\Gamma}. \end{aligned} \quad (38)$$

Therefore, the resultant control input $\dot{\mathbf{q}} = \dot{\mathbf{q}}_N + \dot{\mathbf{q}}_S$ is given by

$$\dot{\mathbf{q}} = \sum_{i=1}^{s-\bar{s}} \frac{1}{\sigma_i} \mathbf{n}_i \mathbf{m}_i^T \mathbf{\Gamma} + \sum_{i=s-\bar{s}+1}^s \frac{1-\kappa_s}{\sigma_i} \mathbf{n}_i \mathbf{m}_i^T \mathbf{\Gamma}, \quad (39)$$

showing that only the components of $\dot{\mathbf{q}}_N$ related to the \bar{s} singular values inside the singular region are attenuated by a factor of $1 - \kappa_s$.

(Statement 2) If $\mathbf{q}(0)$ is outside a singular region then $f_{\sigma}(\sigma_{\min}) = 0$ when $t = 0$. Whenever the robot enters a singular region, $f_{\sigma}(\sigma_{\min})$ increases and $\kappa_s = 1$ when $f_{\sigma}(\sigma_{\min}) = 1$. Therefore, the robot is unable to go further in the direction of the singularity because the components of the control inputs belonging to $\text{span}(\mathbf{n}_{s-\bar{s}+1}, \dots, \mathbf{n}_s)$ —which are the ones driving the robot toward the singularity—are multiplied by 0 and hence do not contribute to the final control input, as shown in (39). That means that σ_{\min} cannot decrease

anymore, therefore $f_{\sigma}(\sigma_{\min}) \leq 1$ for all $t \geq 0$. In that case, from (34) we obtain $\sigma_{\min} \geq \sigma_{\text{region}}(1 - \sigma_{\text{far}}^{-1})$.

In addition, from (33) and (38) we obtain

$$\text{vec}_6 \underline{\mathbf{v}}_s = \mathbf{J} \dot{\mathbf{q}}_S = \sum_{i=s-\bar{s}+1}^s -\kappa_s \mathbf{m}_i \mathbf{m}_i^T \mathbf{\Gamma}.$$

As $\|\mathbf{m}_i\| = 1$ for all i , thus

$$\|\text{vec}_6 \underline{\mathbf{v}}_s\| = \kappa_s \left(\sum_{i=s-\bar{s}+1}^s (\mathbf{m}_i^T \mathbf{\Gamma})^2 \right)^{\frac{1}{2}} \leq \kappa_s \sqrt{\bar{s}} \|\mathbf{\Gamma}\|. \quad (40)$$

Since $\bar{s} \leq s \leq 6$, $\kappa_s \leq 1$ and $\mathbf{\Gamma}$ is bounded,⁹ the disturbance $\underline{\mathbf{v}}_s$ is bounded.

(Statement 3) The control input (36) can be rewritten as $\dot{\mathbf{q}} = \dot{\mathbf{q}}_N + \dot{\mathbf{q}}_S$, where $\dot{\mathbf{q}}_N$ is the nominal input given by (31) and $\dot{\mathbf{q}}_S$ is the auxiliary control input (37). By replacing $\dot{\mathbf{q}}$ in (30), we obtain

$$\begin{aligned} \dot{\underline{\mathbf{x}}} &= \frac{1}{2} (\text{vec}_6(\mathbf{J}\dot{\mathbf{q}}_N) + \text{vec}_6(\mathbf{J}\dot{\mathbf{q}}_S) + \underline{\mathbf{v}}_w + \underline{\mathbf{v}}_c) \underline{\mathbf{x}} - \frac{1}{2} \underline{\mathbf{x}} \underline{\mathbf{x}}_{\underline{\mathbf{d}}} \\ &= \frac{1}{2} (\text{vec}_6(\mathbf{J}\dot{\mathbf{q}}_N) + \underline{\mathbf{v}}_w + \underline{\mathbf{v}}_c) \underline{\mathbf{x}}, \end{aligned} \quad (41)$$

where $\underline{\mathbf{v}}_w = \underline{\mathbf{v}}_s + \underline{\mathbf{v}}_w$ accounts for exogenous disturbances on the twist and the resulting disturbance from the auxiliary control input, and $\dot{\mathbf{q}}_N = \mathbf{J}^+ \left[\kappa_{\mathcal{O}} (\text{vec}_3 \mathcal{O}(\underline{\mathbf{z}}))^T \quad -\kappa_{\mathcal{T}} (\text{vec}_3 \mathcal{T}(\underline{\mathbf{z}}))^T \right]^T$.¹⁰ Since (41) is the same closed-loop dynamics obtained from (20) under control law (21), the rest of the proof follows exactly the same steps from Theorem 3, as long as $\underline{\mathbf{v}}_w, \underline{\mathbf{v}}_w' \in L_2(0, \infty)$ owing to the requirements of Condition 2 in Definition 2.

Since the sum of square integrable functions is also square-integrable and $\underline{\mathbf{v}}_w = (\underline{\mathbf{v}}_s + \underline{\mathbf{v}}_w) + \varepsilon(\underline{\mathbf{v}}_s' + \underline{\mathbf{v}}_w')$, it suffices to show that $\text{vec}_6 \underline{\mathbf{v}}_s$ is square-integrable to ensure that $\underline{\mathbf{v}}_w, \underline{\mathbf{v}}_w' \in L_2(0, \infty)$. Therefore, as $\mathbf{\Gamma}$ is bounded, if the stable point is not inside the singular region then $\exists t_f$ such that $\kappa_s(t) = 0$, $\forall t > t_f$. Consequently, from (40) and using the fact that $\bar{s} \leq 6$ and $0 \leq \kappa_s \leq 1$, we obtain

$$\begin{aligned} \int_0^{\infty} \|\text{vec}_6 \underline{\mathbf{v}}_s\|^2 dt &= \int_0^{t_f} \|\text{vec}_6 \underline{\mathbf{v}}_s\|^2 dt \\ &\leq 6 \int_0^{t_f} \kappa_s^2 \|\mathbf{\Gamma}\|^2 dt < \infty, \end{aligned}$$

which concludes the proof. \blacksquare

IV. SIMULATION RESULTS

In order to validate and quantitatively assess the performance of the proposed techniques, we implemented all control schemes under different conditions and objectives. This section presents the obtained results based on V-REP¹¹ simulations with Bullet 2.83 physics engine running in default asynchronous mode, using a KUKA LBR-IV arm connected

⁹Assuming that $\underline{\mathbf{x}}_{\underline{\mathbf{d}}}$ is bounded.

¹⁰The right pseudoinverse is defined in this case owing to the assumption that $\mathbf{q}(0)$ is outside the singular region and because there exists a lower bound for σ_{\min} according to Statement 2.

¹¹Virtual Robot Experimentation Platform from Coppelia Robotics GmbH

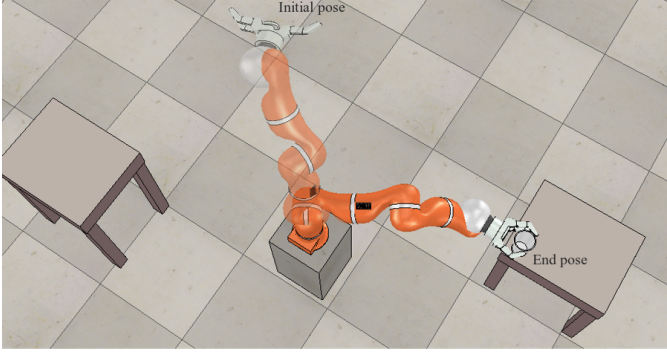


Figure 1: Screenshot from the set-point control task in V-REP.

to a Barrett Hand. The sampling period was 5 ms and the DQ Robotics toolbox¹² was used for both robot modeling and control using dual quaternion algebra.

A. Setpoint control

For the first scenario, the initial manipulator end-effector pose was given by $\underline{\mathbf{x}}_0 = \mathbf{r}_0 + (1/2)\varepsilon\mathbf{p}_0\mathbf{r}_0$, with $\mathbf{r}_0 = \cos(\phi_0/2)\hat{\mathbf{i}} + \mathbf{n}_0 \sin(\phi_0/2)$ such that $\phi_0 = 2.187$ rad and $\mathbf{n}_0 = -0.689\hat{\mathbf{i}} + 0.395\hat{\mathbf{j}} + 0.606\hat{\mathbf{k}}$, from where it was supposed to travel to $\underline{\mathbf{x}}_d = \mathbf{r}_d + (1/2)\varepsilon\mathbf{p}_d\mathbf{r}_d$ with $\mathbf{r}_d = \cos(\pi/4)\hat{\mathbf{i}} + \hat{\mathbf{j}}\sin(\pi/4)$ and $\mathbf{p}_d = 1.56\hat{\mathbf{i}} - 0.43\hat{\mathbf{j}} + 0.65\hat{\mathbf{k}}$ in order to grasp a cup. The initial and final robot configurations are illustrated in Fig. 1.

In order to evaluate our proposed technique in a regulation problem, we compared the control law (21) from Theorem 3 to three controllers based on dual quaternion representation:

- 1) The controller from [13]: $\dot{\mathbf{q}} = \mathbf{J}_{R_8}^+ \kappa \text{vec}_8(\underline{\mathbf{x}}_d - \underline{\mathbf{x}})$, where $\text{vec}_8 : \mathcal{H} \rightarrow \mathbb{R}^8$ and $\text{vec}_8 \underline{\mathbf{x}} = \mathbf{J}_{R_8} \dot{\mathbf{q}}$;¹³
- 2) The controller from [14]: $\dot{\mathbf{q}} = \mathbf{N}_{R_8}^+ \kappa \text{vec}_8(1 - \underline{\mathbf{x}}^* \underline{\mathbf{x}}_d)$, where $\mathbf{N}_{R_8} = \bar{\mathbf{H}}(\underline{\mathbf{x}}_d) \mathbf{C}_8 \mathbf{J}_{R_8}$ with $\bar{\mathbf{H}}(\cdot)$ being the matrix that satisfies $\text{vec}_8(\underline{\mathbf{a}}\underline{\mathbf{b}}) = \bar{\mathbf{H}}(\underline{\mathbf{b}}) \text{vec}_8 \underline{\mathbf{a}}$ for $\underline{\mathbf{a}}, \underline{\mathbf{b}} \in \mathcal{H}$ and $\mathbf{C}_8 = \text{diag}(1, -1, -1, -1, 1, -1, -1, -1)$;
- 3) Decoupled controller that concerns independent attitude and translation task Jacobians:

$$\dot{\mathbf{q}} = \mathbf{J}_{\text{dec}}^+ \kappa \begin{bmatrix} \text{vec}_3(\underline{\mathbf{p}}_d - \underline{\mathbf{p}}) \\ \text{vec}_4(1 - \underline{\mathbf{r}}^* \underline{\mathbf{r}}_d) \end{bmatrix}, \quad \text{with } \mathbf{J}_{\text{dec}} = \begin{bmatrix} \mathbf{J}_p \\ \mathbf{N}_{R_4} \end{bmatrix}$$

where $\text{vec}_4 : \mathbb{H} \rightarrow \mathbb{R}^4$, analogously to (7), $\text{vec}_3 \dot{\underline{\mathbf{p}}} = \mathbf{J}_p \dot{\mathbf{q}}$ and \mathbf{N}_{R_4} corresponds to the four upper rows of \mathbf{N}_{R_8} .

To allow a fair comparison, all controllers were set with the same constant control gain $\kappa_{\mathcal{O}} = \kappa_{\mathcal{T}} = \kappa = 2$.

The error norm in Fig. 2 shows similar convergence behavior for all controllers, as expected for undisturbed scenarios, because all of them ensure the same exponential error decay as they have the same gain. In contrast, the norm of the control input (i.e., the instantaneous control effort), shown in Fig. 3, presents higher peaks for the decoupled controller whereas the controller from Theorem 3 requires the least amount of control effort. Although all controllers have the same gain (which ensures the same convergence rate), they

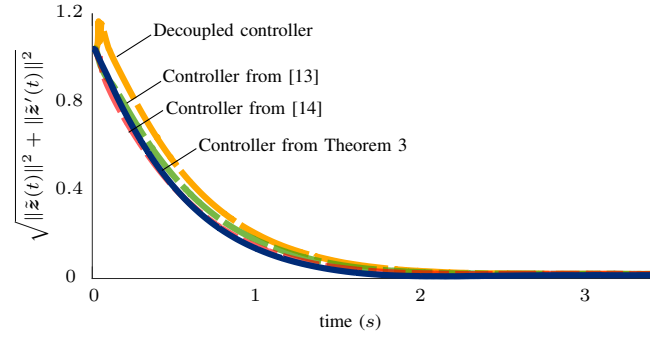


Figure 2: Setpoint control error.

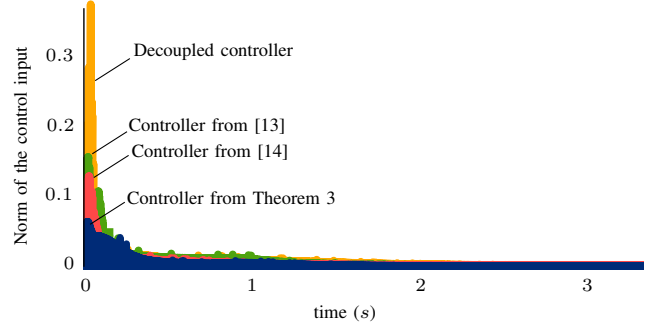


Figure 3: Setpoint control: norm of the control input.

employ different error metrics, hence resulting in different end-effector trajectories, which in turn require different control efforts.

B. Tracking

After grasping the cup, the end-effector was prescribed to follow a desired task trajectory to bring the cup towards the end-pose $\underline{\mathbf{x}}_d(t_f)$, which is located on the top of the left table in Fig. 1, given by with $\mathbf{r}_d(t_f) = 0.67\hat{\mathbf{i}} + 0.01\hat{\mathbf{j}} - 0.74\hat{\mathbf{k}}$ and $\mathbf{p}_d(t_f) = 0.05\hat{\mathbf{i}} - 1.15\hat{\mathbf{j}} + 0.75\hat{\mathbf{k}}$. In order to evaluate our proposed tracking trajectory controller, we compared both Theorems 3 and 4, where the latter has the feedforward correction from the desired end-effector twist.

The trajectory tracking error is shown in Fig. 4. The curves depicted in blue concerns the results based on the tracking control law of Theorem 4 with a small gain $\kappa = 1$ (light dashed-blue) and $\kappa = 5$ (solid blue), whereas the curves in red represents the results from the set-point controller of Theorem 3 with the same gains; that is, $\kappa = 1$ (light dashed red) and $\kappa = 5$ (solid red). The error difference between both controllers, for both control gains, highlights the importance of using the feedforward during tracking control.

C. H_∞ robustness

To illustrate the performance of the proposed robust H_∞ controller under different uncertainties and disturbances, the cup was mounted on a mobile platform, a Pioneer P3-DX from Adept Mobile Robots LCC, which moved in triangle-wave fashion, alternating smoothly back and forth at fixed speed (respectively with period of 2.5 s and 3.45 s), and the end-effector had to track the non-fixed target with a constant

¹²<http://dqrobotics.sourceforge.net>

¹³The operators vec_8 and vec_4 are analogous to (7).

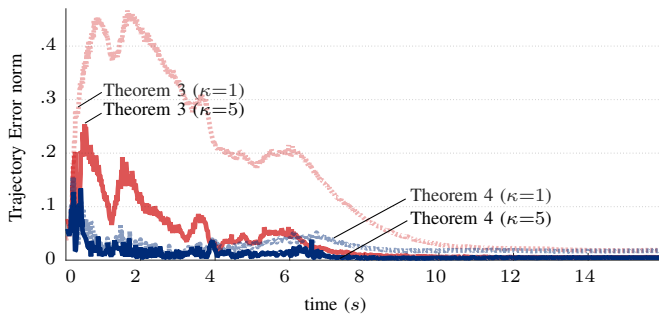


Figure 4: Tracking error: the *blue* and *light-blue* lines correspond to the control law based on Theorem 4; the *red* and *light-red* lines correspond to the setpoint control law of Theorem 3.

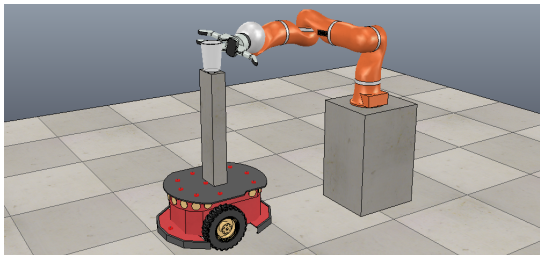


Figure 5: The end-effector must maintain a constant pose with respect to the cup. As the mobile robot follows an unknown trajectory, the corresponding cup velocity is also unknown and is regarded as a disturbance that directly affects the end-effector pose.

relative pose (see Fig. 5). Since in this scenario the robot manipulator does not have knowledge of the mobile base velocity, the cup has a corresponding unknown twist, which is a disturbance that directly affects the relative pose.

Since the cup trajectory is unknown, we used Theorem 3 (setpoint control) with $\gamma_{\mathcal{T}} = \gamma_{\mathcal{T}1} = \gamma_{\mathcal{T}2}$ and $\gamma_{\mathcal{O}} = \gamma_{\mathcal{O}1} = \gamma_{\mathcal{O}2}$. Different values for $\gamma_{\mathcal{T}}$ were used while $\gamma_{\mathcal{O}} = 2$. Table I summarizes the numerically computed noise to error attenuation,

$$\gamma_{\mathcal{T} \text{ sim}} = \frac{\int_0^T \|\mathcal{S}(\tilde{\mathbf{z}}(t))\|^2 dt}{\int_0^T \|\mathbf{v}'_w(t)\|^2 + \|\mathbf{v}'_c(t)\|^2 dt}, \quad \gamma_{\mathcal{O} \text{ sim}} = \frac{\int_0^T \|\mathcal{A}(\tilde{\mathbf{z}}(t))\|^2 dt}{\int_0^T \|\mathbf{v}_w(t)\|^2 + \|\mathbf{v}_c(t)\|^2 dt}.$$

As expected from the H_{∞} norm given by Definition 2, the noise to error attenuation remains below the prescribed threshold values, that is, $\gamma_{\mathcal{O} \text{ sim}} \leq \gamma_{\mathcal{O}}$ and $\gamma_{\mathcal{T} \text{ sim}} \leq \gamma_{\mathcal{T}}$, for all $\gamma_{\mathcal{O}}$ and $\gamma_{\mathcal{T}}$.

Figure 6 shows the relative pose error along time for $\gamma_{\mathcal{T}} = \{0.5, 2, 3.5\}$ and $\gamma_{\mathcal{O}} = 2$ with the same disturbances acting on the system (i.e., the same unknown cup velocities). As the theory predicts, smaller values of $\gamma_{\mathcal{T}}$ and $\gamma_{\mathcal{O}}$ result in more disturbance attenuation and, consequently, less error.

The proposed controller (Theorem 3 with $\gamma_{\mathcal{T}}=0.4$, $\gamma_{\mathcal{O}}=1$) was again compared to the controllers from [13] and [14], which were described in Section IV-A. To maintain fairness, all controllers were manually set to ensure similar control effort in terms of $\int_0^T \|\mathbf{u}(t)\| dt$. The numerically calculated noise-to-error attenuation from the simulations, presented in

Table I: Comparison between theoretical upper bound ($\gamma_{\mathcal{T}}$, $\gamma_{\mathcal{O}}$) with the numerically calculated noise-to-error attenuation from simulation ($\gamma_{\mathcal{T} \text{ sim}}$, $\gamma_{\mathcal{O} \text{ sim}}$).

$\gamma_{\mathcal{T}}$	3.5	2.0	0.9	0.6	0.5	0.4	0.2
$\gamma_{\mathcal{T} \text{ sim}}$	1.914	1.235	0.736	0.528	0.404	0.326	0.167
$\gamma_{\mathcal{O}}$	2	2	2	2	2	2	2
$\gamma_{\mathcal{O} \text{ sim}}$	0.95	1.01	0.99	1.03	1.04	1.01	0.99

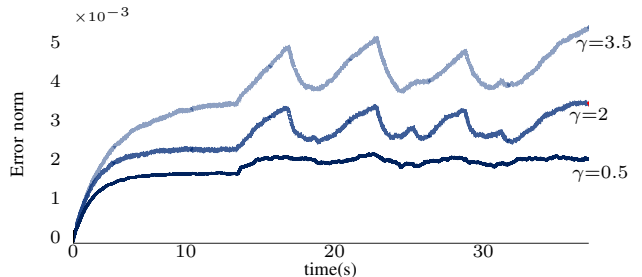


Figure 6: Control error for $\gamma_{\mathcal{O}} = 2$ and different values of the prescribed noise-to-error upper bound $\gamma_{\mathcal{T}}$.

Table II, shows that for the same control effort our controller outperforms the other ones in terms of disturbance attenuation.

D. H_{∞} -based Singularity Avoidance

In the last scenario, the cup is placed outside the end-effector workspace in order to induce inescapable singularities. The robot starts and ends in non-singular configurations, but reaching for the cup causes a full extension of the arm, which results in singular configurations from $t \geq 2$ s. From $t=6$ s to $t=7.5$ s, the desired trajectory remains constant, as if the task was completed, then the end-effector is driven to the opposite direction, back to the initial pose, reaching the non-singular configuration at $t = 9.5$ s.

Since the lack of singularity avoidance causes large accelerations and chattering in the vicinity of such configurations (or even unstable behavior), we used Theorem 6 and compared to the damped least-squares inverse [16] with adaptive damping-rate [18], which is widely used in robotics. This adaptive damped least-squares inverse (ALSI) was implemented in the pseudoinverse of Theorem 4. Both avoidance algorithms are naturally sensitive to parameters selection, but we chose the same limit for the singular region; that is, $\sigma_{\text{region}} = \epsilon = 10^{-2}$ and $\sigma_{\text{far}} = \lambda_{\text{max}} = 2$, where ϵ , λ_{max} are the parameters required for ALSI [18].

The error norm and instantaneous control effort (i.e., norm of the control inputs) along the trajectory are shown in Fig. 7, showing that our proposed method outperforms ALSI both in terms of tracking error and control effort. Furthermore, the figure in the bottom of Fig. 7 shows that the least singular value is always greater or equal than $\sigma_{\text{region}} (1 - \sigma_{\text{far}}^{-1}) = 0.005$, as predicted by the second statement in Theorem 6. In addition,

Table II: Comparison between numerically calculated noise-to-error attenuation ($\gamma_{\mathcal{T} \text{ sim}}$, $\gamma_{\mathcal{O} \text{ sim}}$) from different simulations.

	Theorem 3	Controller [14]	Controller [13]
$\gamma_{\mathcal{T}} = 0.4$	$\gamma_{\mathcal{T} \text{ sim}} = 0.32$	$\gamma_{\mathcal{T} \text{ sim}} = 0.63$	$\gamma_{\mathcal{T} \text{ sim}} = 0.61$
$\gamma_{\mathcal{O}} = 1.0$	$\gamma_{\mathcal{O} \text{ sim}} = 0.65$	$\gamma_{\mathcal{O} \text{ sim}} = 0.86$	$\gamma_{\mathcal{O} \text{ sim}} = 0.87$

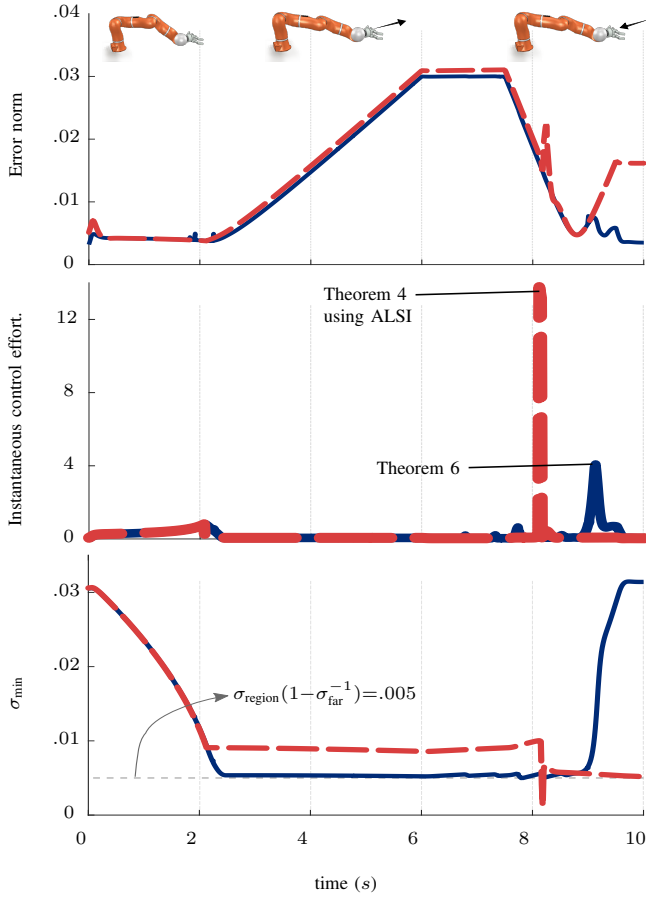


Figure 7: Tracking in the presence of singularities: Theorem 4 with adaptive damped least-squares inverse [18] (*red dashed lines*) versus Theorem 6 (*solid blue lines*).

in this example ALSI was more conservative than our method most of the time (i.e., it did not get sufficiently close to the singular region), which is undesirable as it may result in worse tracking error, as shown in Fig. 7, although it briefly violated the prescribed value for the smaller singular value at around $t = 8$ s.

V. CONCLUSIONS

This paper proposes a novel robust motion control strategy for robot manipulators based on dual quaternion algebra and the H_∞ theory. With a detailed investigation on sources and effects of uncertainties and disturbances in the robot differential kinematics, which is described using dual quaternion algebra, we derived an explicit connection between their detrimental influence and performance over the end-effector trajectory in the H_∞ sense. Exploiting the geometrical significance of the dual quaternion algebra, we adapted classic H_∞ solutions—which concern solely additive noises—to derive an easy-to-implement closed-form H_∞ controller. This controller incorporates explicit robustness and performance specifications while minimizing the instantaneous control effort for the required performance design.

Moreover, to ensure proper behavior and closed-loop stability throughout the whole task space, including the workspace

boundary, the proposed H_∞ strategy was extended to avoid any kind of singularity while providing formal guarantees that singularities have limited effect on the end-effector trajectory.

Simulations on a realistic simulator were performed in different conditions and with different control strategies, which led to the following conclusions: *a)* the proposed controller require less instantaneous control effort (which implies less kinetic energy), when no disturbances affect the system, compared to similar controllers with same convergence rate and settling time; *b)* when there are disturbances, if all controllers are tuned to have similar control effort, our controller ensures less setpoint and tracking errors; *c)* in the presence of singularities, our controller outperforms the ones based on the adaptive damped least-square inverse, which are widely used in the literature, both in terms of control effort and tracking errors, while bounding the minimal singular value to the prescribed value.

APPENDIX

DERIVATIVE OF LYAPUNOV FUNCTION (22)

Let us recall that, from (15), $\tilde{\mathbf{z}} \triangleq 1 - \tilde{\mathbf{x}} = \tilde{\mathbf{z}} + \varepsilon \tilde{\mathbf{z}}'$. By letting $\tilde{\mathbf{x}} \triangleq \boldsymbol{\eta} + \boldsymbol{\mu} + \varepsilon (\boldsymbol{\eta}' + \boldsymbol{\mu}')$, the positive definite functions V_1 and V_2 in the Lyapunov function (22) can be rewritten as

$$\begin{aligned} V_1(t, \tilde{\mathbf{z}}) &= \alpha_1 \|\tilde{\mathbf{z}}(t)\|^2 \\ &= \alpha_1 \left((1 - \eta)^2 + \|\boldsymbol{\mu}\|_2^2 \right) \\ &= 2\alpha_1 (1 - \eta), \end{aligned}$$

and

$$V_2(t, \tilde{\mathbf{z}}') = \alpha_2 \|\tilde{\mathbf{z}}'(t)\|^2 = \alpha_2 \left(\eta'^2 + \|\boldsymbol{\mu}'\|^2 \right).$$

Taking the time-derivative of (22) yields $\dot{V}(t, \tilde{\mathbf{z}}) = \dot{V}_1(t, \tilde{\mathbf{z}}) + \dot{V}_2(t, \tilde{\mathbf{z}}')$ with

$$\begin{aligned} \dot{V}_1(t, \tilde{\mathbf{z}}) &= -2\alpha_1 \dot{\eta}, \\ \dot{V}_2(t, \tilde{\mathbf{z}}') &= 2\alpha_2 \eta' \dot{\eta}' + 2\alpha_2 \langle \boldsymbol{\mu}', \dot{\boldsymbol{\mu}}' \rangle. \end{aligned}$$

Using the control law (21) in (20),¹⁴ we obtain¹⁵

$$\begin{aligned} \dot{\eta} &= -\frac{1}{2} \langle \mathbf{h}_1, \boldsymbol{\mu} \rangle, \\ \dot{\eta}' &= -\frac{1}{2} (\langle \mathbf{h}_1, \boldsymbol{\mu}' \rangle + \langle \mathbf{h}_2, \boldsymbol{\mu} \rangle), \\ \dot{\boldsymbol{\mu}}' &= \frac{1}{2} (\eta' \mathbf{h}_1 + \eta \mathbf{h}_2 + \mathbf{h}_1 \times \boldsymbol{\mu}' + \mathbf{h}_2 \times \boldsymbol{\mu}), \end{aligned}$$

where

$$\begin{aligned} \mathbf{h}_1 &= \kappa_{\mathcal{O}} \mathcal{O}(\tilde{\mathbf{z}}) + \mathbf{v}_w + \mathbf{v}_c, \\ \mathbf{h}_2 &= -\kappa_{\mathcal{T}} \mathcal{T}(\tilde{\mathbf{z}}) + \mathbf{v}'_w + \mathbf{v}'_c. \end{aligned}$$

¹⁴Those equations hold even if \mathbf{J} is not full row rank (hence $\mathbf{J}\mathbf{J}^+ \neq \mathbf{I}$), which usually happens when there is a kinematic singularity. In that case, let $\mathbf{s} \triangleq [\kappa_{\mathcal{O}} (\text{vec}_3 \mathcal{O}(\tilde{\mathbf{z}}))^T \quad -\kappa_{\mathcal{T}} (\text{vec}_3 \mathcal{T}(\tilde{\mathbf{z}}))^T]^T$ then $\text{vec}_6(\mathbf{J}\mathbf{J}^+ \mathbf{s}) = \text{vec}_6(\mathbf{s}) + \underline{\mathbf{v}}_s$, where $\underline{\mathbf{v}}_s = \mathbf{v}_s + \varepsilon \mathbf{v}'_s$ is a disturbance to be added into $\underline{\mathbf{v}}_w$. In such case, one must ensure that $\mathbf{v}_s, \mathbf{v}'_s \in L_2[0, \infty)$ as shown in Theorem 6.

¹⁵In those calculations, we use the fact that given $\mathbf{u}, \mathbf{v} \in \mathbb{H}_p$, $\mathbf{u}\mathbf{v} = -\langle \mathbf{u}, \mathbf{v} \rangle + \mathbf{u} \times \mathbf{v}$, which is easy to see from (3).

Hence,

$$\dot{V}_1(t, \tilde{\mathbf{z}}) = \alpha_1 \langle \mathbf{h}_1, \boldsymbol{\mu} \rangle \quad (42)$$

$$\begin{aligned} \dot{V}_2(t, \tilde{\mathbf{z}}') &= -\alpha_2 \eta' (\langle \mathbf{h}_1, \boldsymbol{\mu}' \rangle + \langle \mathbf{h}_2, \boldsymbol{\mu} \rangle) \\ &\quad + \alpha_2 \langle \boldsymbol{\mu}', (\eta' \mathbf{h}_1 + \eta \mathbf{h}_2 + \mathbf{h}_1 \times \boldsymbol{\mu}' + \mathbf{h}_2 \times \boldsymbol{\mu}) \rangle \\ &= -\alpha_2 \eta' \langle \boldsymbol{\mu}, \mathbf{h}_2 \rangle + \alpha_2 \langle \boldsymbol{\mu}', \eta \mathbf{h}_2 \rangle \\ &\quad + \alpha_2 \langle \boldsymbol{\mu}', (\mathbf{h}_1 \times \boldsymbol{\mu}') \rangle + \alpha_2 \langle \boldsymbol{\mu}', (\mathbf{h}_2 \times \boldsymbol{\mu}) \rangle \\ &= \alpha_2 \langle \eta \boldsymbol{\mu}' - \eta' \boldsymbol{\mu}, \mathbf{h}_2 \rangle + \alpha_2 \langle \boldsymbol{\mu}, \boldsymbol{\mu}' \times \mathbf{h}_2 \rangle \\ &= \alpha_2 \langle \eta \boldsymbol{\mu}' - \eta' \boldsymbol{\mu} + \boldsymbol{\mu} \times \boldsymbol{\mu}', \mathbf{h}_2 \rangle. \end{aligned} \quad (43)$$

To investigate the first condition from Definition 2, which regards exponential stability of (19) in the absence of disturbances $\underline{\mathbf{v}}_w$ and $\underline{\mathbf{v}}_c$, let us rewrite (42)-(43) as $\dot{V}(t, \tilde{\mathbf{z}}) = \dot{V}_1(t, \tilde{\mathbf{z}}) + \dot{V}_2(t, \tilde{\mathbf{z}}')$ with

$$\begin{aligned} \dot{V}_1(t, \tilde{\mathbf{z}}) &= \alpha_1 \langle \boldsymbol{\mu}, \kappa_{\mathcal{O}} \mathcal{O}(\tilde{\mathbf{z}}) \rangle \\ \dot{V}_2(t, \tilde{\mathbf{z}}') &= -\alpha_2 \langle \eta \boldsymbol{\mu}' - \eta' \boldsymbol{\mu} + \boldsymbol{\mu} \times \boldsymbol{\mu}', \kappa_{\mathcal{T}} \mathcal{T}(\tilde{\mathbf{z}}) \rangle. \end{aligned}$$

Noting that $\mathcal{T}(\tilde{\mathbf{z}}) = 2(\eta \boldsymbol{\mu}' - \eta' \boldsymbol{\mu} + \boldsymbol{\mu} \times \boldsymbol{\mu}')$ and $\mathcal{O}(\tilde{\mathbf{z}}) = -\boldsymbol{\mu}$ (see Remark 1), we have

$$\begin{aligned} \dot{V}_1(t, \tilde{\mathbf{z}}) &= -\alpha_1 \kappa_{\mathcal{O}} \langle \boldsymbol{\mu}, \boldsymbol{\mu} \rangle, \\ \dot{V}_2(t, \tilde{\mathbf{z}}') &= -2\alpha_2 \kappa_{\mathcal{T}} \langle \eta \boldsymbol{\mu}' - \eta' \boldsymbol{\mu} + \boldsymbol{\mu} \times \boldsymbol{\mu}', \eta \boldsymbol{\mu}' - \eta' \boldsymbol{\mu} + \boldsymbol{\mu} \times \boldsymbol{\mu}' \rangle \\ &= -2\alpha_2 \kappa_{\mathcal{T}} \left(\eta^2 \langle \boldsymbol{\mu}', \boldsymbol{\mu}' \rangle + \eta'^2 \langle \boldsymbol{\mu}, \boldsymbol{\mu} \rangle - 2\eta \eta' \langle \boldsymbol{\mu}, \boldsymbol{\mu}' \rangle \right. \\ &\quad \left. + \langle \boldsymbol{\mu}, \boldsymbol{\mu} \rangle \langle \boldsymbol{\mu}', \boldsymbol{\mu}' \rangle - \langle \boldsymbol{\mu}, \boldsymbol{\mu}' \rangle^2 \right). \end{aligned}$$

From the unit dual quaternion group constraint (4), $\eta \eta' + \langle \mathbf{u}, \mathbf{u}' \rangle = 0$ [33], we obtain

$$\begin{aligned} \dot{V}_1(t, \tilde{\mathbf{z}}) &= -\alpha_1 \kappa_{\mathcal{O}} \|\boldsymbol{\mu}\|^2 = -\alpha_1 \kappa_{\mathcal{O}} \frac{1}{2} (\|\boldsymbol{\mu}\|^2 + \|\boldsymbol{\mu}\|^2) \\ &= -\alpha_1 \frac{\kappa_{\mathcal{O}}}{2} (1 - \eta^2 + \|\boldsymbol{\mu}\|^2) \\ \dot{V}_2(t, \tilde{\mathbf{z}}') &= -2\alpha_2 \kappa_{\mathcal{T}} \left(\eta^2 \|\boldsymbol{\mu}'\|^2 + \eta'^2 \|\boldsymbol{\mu}\|^2 - 2\eta \eta' (-\eta \eta') \right. \\ &\quad \left. + \|\boldsymbol{\mu}\|^2 \|\boldsymbol{\mu}'\|^2 - (-\eta \eta')^2 \right) \\ &= -2\alpha_2 \kappa_{\mathcal{T}} \left(\eta^2 \|\boldsymbol{\mu}'\|^2 + \eta'^2 \|\boldsymbol{\mu}\|^2 + \eta^2 \eta'^2 + (1 - \eta^2) \|\boldsymbol{\mu}'\|^2 \right) \\ &= -2\alpha_2 \kappa_{\mathcal{T}} \left(\|\boldsymbol{\mu}'\|^2 + \eta'^2 (1 - \eta^2) + \eta^2 \eta'^2 \right) \\ &= -2\alpha_2 \kappa_{\mathcal{T}} \left(\eta'^2 + \|\boldsymbol{\mu}'\|^2 \right) = -2\alpha_2 \kappa_{\mathcal{T}} \|\tilde{\mathbf{z}}'(t)\|^2. \end{aligned} \quad (44)$$

For $\eta \in [0, 1]$, it is easy to see that $(1 - \eta)^2 \leq (1 - \eta^2)$. Hence,

$$\dot{V}_1(t, \tilde{\mathbf{z}}) \leq -\alpha_1 \frac{\kappa_{\mathcal{O}}}{2} \left((1 - \eta)^2 + \|\boldsymbol{\mu}\|^2 \right) = -\alpha_1 \frac{\kappa_{\mathcal{O}}}{2} \|\tilde{\mathbf{z}}(t)\|^2, \quad (45)$$

thus

$$\dot{V}(t, \tilde{\mathbf{z}}) \leq -\alpha_1 \frac{\kappa_{\mathcal{O}}}{2} \|\tilde{\mathbf{z}}(t)\|^2 - 2\alpha_2 \kappa_{\mathcal{T}} \|\tilde{\mathbf{z}}'(t)\|^2,$$

which in turn yields (23).

Remark 7. To address the interval $\eta \in [-1, 0]$ and prevent the problem of unwinding [33], one must assume $\tilde{\mathbf{z}} = 1 + \tilde{\mathbf{x}}$ instead of (15). Hence, without loss of generality, the exact same controller from Theorem 3 yields (23) with $\|\tilde{\mathbf{z}}(t)\|^2 = (1 + \eta)^2 + \|\boldsymbol{\mu}\|^2$ where $\eta = -1$ is the equilibrium.¹⁶

¹⁶One must only observe that $\mathcal{O}(\tilde{\mathbf{z}}) = \boldsymbol{\mu}$ when $\tilde{\mathbf{z}} = 1 + \tilde{\mathbf{x}}$, and the inequality $(1 + \eta)^2 \leq 1 - \eta^2$ holds when $\eta \in [-1, 0]$.

Now, if we explicitly regard the influence of $\underline{\mathbf{v}}_w$ and $\underline{\mathbf{v}}_c$, the Lyapunov derivative (42)-(43) yields¹⁷

$$\begin{aligned} \dot{V}(t, \tilde{\mathbf{z}}) &= -\alpha_1 \langle \mathcal{O}(\tilde{\mathbf{z}}), \kappa_{\mathcal{O}} \mathcal{O}(\tilde{\mathbf{z}}) + \mathbf{v}_w + \mathbf{v}_c \rangle \\ &\quad + \frac{\alpha_2}{2} \langle \mathcal{T}(\tilde{\mathbf{z}}), -\kappa_{\mathcal{T}} \mathcal{T}(\tilde{\mathbf{z}}) + \mathbf{v}'_w + \mathbf{v}'_c \rangle, \end{aligned} \quad (46)$$

which is equivalent to (24).

REFERENCES

- [1] R. Alami, A. Albu-Schaeffer, A. Bicchi, R. Bischoff, R. Chatila, A. De Luca, A. De Santis, G. Giralt, J. Guiochet, G. Hirzinger, F. Ingrand, V. Lippiello, R. Mattone, D. Powell, S. Sen, B. Siciliano, G. Tonietti, and L. Villani, "Safe and dependable physical human-robot interaction in anthropic domains: State of the art and challenges," in *2006 IEEE/RSJ International Conference on Intelligent Robots and Systems*, vol. 6, no. 1. IEEE, oct 2006, pp. 1–16.
- [2] B. Siciliano, L. Sciacivco, L. Villani, and G. Oriolo, *Robotics: modelling, planning and control*. Springer Verlag, 2009.
- [3] B. V. Adorno, "Two-arm manipulation: From manipulators to enhanced human-robot collaboration," Ph.D. dissertation, Laboratoire d'Informatique, de Robotique et de Microélectronique de Montpellier (LIRMM) - Université Montpellier 2, Montpellier, France, 2011.
- [4] X. Wang and H. Zhu, "On the Comparisons of Unit Dual Quaternion and Homogeneous Transformation Matrix," *Advances in Applied Clifford Algebras*, vol. 24, no. 1, pp. 213–229, dec 2013. [Online]. Available: <http://link.springer.com/10.1007/s00006-013-0436-y>
- [5] N. A. Aspragathos and J. K. Dimitros, "A Comparative Study of Three Methods for Robot Kinematics," *IEEE Transactions on Systems, Man, and Cybernetics, Part B: Cybernetics*, vol. 28, no. 2, pp. 135–145, 1998.
- [6] L. A. Radavelli, E. R. D. Pieri, D. Martins, and R. Simoni, "Points, Lines, Screws and Planes in Dual Quaternions Kinematics," in *Advances in Robot Kinematics*, J. Lenarčič and O. Khatib, Eds. Cham: Springer International Publishing, 2014, pp. 285–293. [Online]. Available: <http://link.springer.com/10.1007/978-3-319-06698-1>
- [7] B. V. Adorno, "Robot Kinematic Modeling and Control Based on Dual Quaternion Algebra – Part I: Fundamentals," 2017. [Online]. Available: <https://hal.archives-ouvertes.fr/hal-01478225v1>
- [8] D.-P. Han, Q. Wei, and Z.-X. Li, "Kinematic control of free rigid bodies using dual quaternions," *International Journal of Automation and Computing*, vol. 5, no. 3, pp. 319–324, 2008.
- [9] X. Wang, D. Han, C. Yu, and Z. Zheng, "The geometric structure of unit dual quaternion with application in kinematic control," *Journal of Mathematical Analysis and Applications*, vol. 389, no. 2, pp. 1352–1364, May 2012.
- [10] X. Wang, C. Yu, and Z. Lin, "A Dual Quaternion Solution to Attitude and Position Control for Rigid-Body Coordination," *IEEE Transactions on Robotics*, vol. 28, no. 5, pp. 1162–1170, 2012.
- [11] X. Wang and C. Yu, "Unit dual quaternion-based feedback linearization tracking problem for attitude and position dynamics," *Systems & Control Letters*, vol. 62, no. 3, pp. 225–233, Mar. 2013.
- [12] I. Mas and C. Kitts, "Quaternions and Dual Quaternions: Singularity-Free Multirobot Formation Control," *Journal of Intelligent & Robotic Systems*, vol. 87, no. 3–4, pp. 643–660, sep 2017. [Online]. Available: <http://link.springer.com/10.1007/s10846-016-0445-x>
- [13] B. V. Adorno, P. Fraise, and S. Druon, "Dual position control strategies using the cooperative dual task-space framework," in *IEEE/RSJ International Conference on Intelligent Robots and Systems*, Taipei, Oct. 2010, pp. 3955–3960.
- [14] L. Figueredo, B. Adorno, J. Ishihara, and G. Borges, "Robust kinematic control of manipulator robots using dual quaternion representation," in *IEEE International Conference on Robotics and Automation (ICRA)*, 2013, pp. 1949–1955.
- [15] B. V. Adorno, a. P. L. Bó, and P. Fraise, "Kinematic modeling and control for human-robot cooperation considering different interaction roles," *Robotica*, vol. 33, no. 2, pp. 314–331, Feb. 2015.
- [16] Y. Nakamura and H. Hanafusa, "Inverse Kinematic Solutions With Singularity Robustness for Robot Manipulator Control," *Journal of Dynamic Systems, Measurement, and Control*, vol. 108, no. 3, p. 163, 1986.

¹⁷Recall that $\mathcal{T}(\tilde{\mathbf{z}}) = 2(\eta \boldsymbol{\mu}' - \eta' \boldsymbol{\mu} + \boldsymbol{\mu} \times \boldsymbol{\mu}')$ and $\mathcal{O}(\tilde{\mathbf{z}}) = -\boldsymbol{\mu}$.

- [17] O. Egeland, J. Sagli, I. Spangelo, and S. Chiaverini, "A damped least-squares solution to redundancy resolution," in *Robotics and Automation, 1991. Proceedings., 1991 IEEE International Conference on*, 1991, pp. 945–950 vol.1.
- [18] S. Chiaverini, "Singularity-robust task-priority redundancy resolution for real-time kinematic control of robot manipulators," *IEEE Transactions on Robotics and Automation*, vol. 13, no. 3, pp. 398–410, Jun. 1997.
- [19] C. Qiu, Q. Cao, and S. Miao, "An on-line task modification method for singularity avoidance of robot manipulators," *Robotica*, vol. 27, no. 4, p. 539, Sep. 2009.
- [20] W. R. Hamilton, "On quaternions, or on a new system of imaginaries in algebra: Copy of a letter from Sir William R. Hamilton to John T. Graves, esq. on quaternions," *Journal of Mechanical Design - Transactions of ASME*, vol. 25, no. 3, pp. 489–495, 1844.
- [21] J. M. Selig, *Geometric fundamentals of robotics*, 2nd ed., D. Gries and F. B. Schneider, Eds. Springer-Verlag New York Inc., 2005. [Online]. Available: <http://www.amazon.fr/Geometric-Fundamentals-Robotics-J-Selig/dp/0387208747>
- [22] J. Kuipers, *Quaternions and Rotation Sequences: A Primer with Applications to Orbits, Aerospace, and Virtual Reality*. Princeton University Press, 1999.
- [23] C. Scherer, "The riccati inequality and state-space H_∞ -optimal control," Ph.D. dissertation, University of Würzburg, Germany, 1990.
- [24] D. Simon, *Optimal State Estimation: Kalman, H_∞ , and Nonlinear approaches*. Wiley-Interscience, 2006.
- [25] H. Khalil, *Nonlinear Systems*, 2nd ed. New Jersey: Prentice-Hall, 1996.
- [26] N. Bedrossian, "Classification of singular configurations for redundant manipulators," in *IEEE International Conference on Robotics and Automation, 1990. Proceedings*, may 1990, pp. 818–823.
- [27] G. Marani, J. Kim, J. Yuh, and W. K. Chung, "Algorithmic singularities avoidance in task-priority based controller for redundant manipulators," in *Proceedings IEEE/RSJ International Conference on Intelligent Robots*, vol. 4, 2003, pp. 3570–3574.
- [28] J. Kim, G. Marani, W. K. Chung, and J. Yuh, "Task reconstruction method for real-time singularity avoidance for robotic manipulators," *Advanced Robotics*, vol. 20, no. 4, pp. 453–481, Jan. 2006.
- [29] —, "A general singularity avoidance framework for robot manipulators: task reconstruction method," in *IEEE International Conference on Robotics and Automation*, 2004.
- [30] R. V. Mayorga and P. Sanongboon, "Inverse kinematics and geometrically bounded singularities prevention of redundant manipulators: An Artificial Neural Network approach," *Robotics and Autonomous Systems*, vol. 53, no. 3-4, pp. 164–176, Dec. 2005.
- [31] O. Bohigas, M. E. Henderson, L. Ros, and J. M. Porta, "A singularity-free path planner for closed-chain manipulators," in *IEEE International Conference on Robotics and Automation*, 2012, pp. 2128–2134.
- [32] M. Spong, S. Hutchinson, and M. Vidyasagar, *Robot modeling and control*. John Wiley & Sons, 2006.
- [33] H. T. Kussaba, L. F. Figueredo, J. Y. Ishihara, and B. V. Adorno, "Hybrid kinematic control for rigid body pose stabilization using dual quaternions," *Journal of the Franklin Institute*, vol. 354, no. 7, pp. 2769–2787, may 2017. [Online]. Available: <http://linkinghub.elsevier.com/retrieve/pii/S0016003217300522>



manipulators, humanoids and cooperative manipulation systems.

Bruno Vilhena Adorno received the BS degree (2005) in Mechatronics Engineering and the MS degree (2008) in Electrical Engineering, both from University of Brasília (Brazil), and the PhD degree (2011) from University of Montpellier (France). He is currently an Assistant Professor with the Department of Electrical Engineering at the Federal University of Minas Gerais (UFMG), Brazil. His current research interests include both practical and theoretical aspects related to robot kinematics, dynamics, and control with applications to mobile



João Y. Ishihara received the Ph.D. degree in Electrical Engineering from the University of São Paulo, Brazil, in 1998. He is currently an Associate Professor at the University of Brasília, Brazil. His research interests include robust filtering and control theory, singular systems, and robotics.



Luis Felipe Cruz Figueredo is a Marie-Sklódowska Curie Research Fellow at the School of Computing, University of Leeds, UK. Previously, he was a postdoctoral fellow at the Federal University of Minas Gerais (UFMG), and a lecturer at University of Brasília (UnB) both in Brazil. He received his MS Degree (2011) in Electrical Engineering and PhD in Control and Robotic Systems from University of Brasília (2016). During 2013-2014, he was a visiting researcher at the MERS group at the Computer Science and Artificial Intelligence Laboratory

(CSAIL) at the Massachusetts Institute of Technology (MIT). Dr Figueredo is enthusiastically engaged in developing novel control and motion planning algorithms for cooperative robots manipulation and human-robot interaction addressing both theoretical and practical aspects of rigid body kinematics and dynamics.